SEISMICITY OF AFAR AND THE MAIN ETHIOPIAN RIFT FROM 2000 - 2002 G.C.

By

Sisay Alemayehu Angere

SUBMITTED IN PARTIAL FULFILLMENT OF THE
REQUIREMENTS FOR THE DEGREE OF
MASTER OF SCIENCE
AT
ADDIS ABABA UNIVERSITY
ADDIS ABABA,ETHIOPIA
JUNE 2011

ADDIS ABABA UNIVERSITY
DEPARTMENT OF
COMPUTATIONAL SCIENCE PROGRAM

The undersigned hereby certify that they have read and recommend to the School of Graduate Studies for acceptance a thesis entitled "**SEISMICITY OF AFAR AND THE MAIN ETHIOPIAN RIFT FROM 2000 - 2002 G.C.**" by **Sisay Alemayehu Angere** in partial fulfillment of the requirements for the degree of **Master of Science**.

Dated: June 2011

Supervisor:

Dr. Atalay Ayele
Advisor

Readers:

Dr. Elias Lewi
Examiner

Dr. Gizaw Mengistu
Examiner

Dr. Lemi Demeyu
Chairperson, Department Graduate Committee

ADDIS ABABA UNIVERSITY

Date: **June 2011**

Author: **Sisay Alemayehu Angere**

Title: **SEISMICITY OF AFAR AND THE MAIN ETHIOPIAN RIFT FROM 2000 - 2002 G.C.**

Department: **Computational Science Program**

Degree: **M.Sc.** Convocation: **June** Year: **2011**

Dedicated to my late mother Mestawet W/Semeyat

Table of Contents

List of Tables

List of Figures

Abstract

Earthquakes data recorded between 2000 and 2002 are used to study the seismicity of Ethiopia mainly focused around Afar and the Main Ethiopian rift. The locations of 238 local earthquake are determined using P- and S- wave arrival times recorded on three or more stations that resulted to a maximum of 1.5 root mean square (RMS). Previous studies of seismicity by Brazier et al., 2006 has been revisited using the same data from IRIS/PASSCAL broadband seismic experiments and adding more from ESSN (Ethiopian Seismic Station Network) sources. Comparing the results in this study with Brazier et al., 2006's, it is found that eight bogus events (earthquakes that didn't occur in the real world) and six more teleseismic earthquakes are reported as if they occurred in the Ethiopian neighborhood. On the other hand, it is observed that Brazier et al's work, which is published in Bulletins of Seismological Society of America (BSSA), reported 25 earthquakes that are located with readings from seismic stations less than three which puts doubt on the accuracy of the seismicity study. Another 53 new earthquakes are identified in the database and located in this study which has improved details of the seismicity of the region for the time period considered.

A Fortran program is written in 0.5 by 0.5 degree window and with 0.5 degree sliding window in order to map the seismic energy release. The distribution of epicenter in this study shows high seismic activity around 9^0N and 40.50^0E; 9.50^0N and 39.50^0E during the study period, these epicenters are close to the N - S trending Ankober region, Kessem area and Dofen volcano. Coda magnitudes are also estimated for the reported events. Similarly b-values are estimated using both the least squares method and the maximum likelihood method. b-value of 0.9 $\pm$ 0.09 and 1.10 were obtained using the maximum-likelihood method and using least square method determined respectively for the highly seismic Ankober-Dofen region during the study period. On the other hand, seismic energy map is developed for the whole region. The relatively high b-value estimated and the seismic energy mapping showed that seismic energy are released in the form of small magnitude.

Acknowledgements

First of all, I would like to thank Almighty God who made it possible for me to begin and finish this work successfully, I am grateful to express my feelings of gratitude to my advisor Dr. Atalay Ayele whose generous guidance and supervision, provision of some necessary materials for the research, encouragement and support throughout the work devoting his valuable time and effort helped me to complete the present research work successfully, I appreciate the effort you made to make me acquainted with research culture. I am also grateful to all staff members of the Institute of Geophysics Space Science and Astronomy especially Dr. Laike Mariam Asfaw, Dr. Elias Lewi, Ato Abebe Albei, Ato Manahloh Belachew and W/o Asnackech Estifanos for providing the friendly and a very pleasant atmosphere right from the start of my career in the Institute.

I would like to thank for all my instructors, especially Dr. Sebsbie Hailemariam, Dr. Semu Mitku, Dr. Berhanu Guta, Dr. Tadese Lemi, Dr. Tsegaye Gedif, Dr. Gizaw Mengistu for their guidance throughout my graduate teaching cources.

I would like to thank all the members of the Computational Science department especially to Dr. Lemi Demeyu and Ato Addisu Gezahegn for their constructive advise and help during difficult time.

This acknowledgment is not enough without thanking Dr. Getnet Mewa, the realization of this work would have been impossible without his encouragement and consistent advise, you are just like big brother to me. I also like to extend my thanks to the following individuals for their financial support: Abgiya's family especially to W/o Kidist Derese and Ato Mulugeta Tekle, Ashenafi Girma, Serkalem Mulunegh, Desta Mola and Birke.

I sincerely thank my beloved family, my brother Besufekad and my sister Kidist for their constructive help and especially my late mother W/o Mestawet W/ Semeyat, who brought me the way I am. Thank you mom for your endless care and love, you are the reason for my success.

Last but not least, I would like to extend my earnest thanks to my classmates especially Tamirat Bekele and colleagues especially to Leta Alemayehu, Yewubinesh Bekele and others who put a drop of contribution in any ways in my study.

CHAPTER 1

Introduction

Computational science (CS) is an emerging new area of specialization that brings computer science and basic sciences together to a new frontier, with numerical computation and graphics visualization playing a key role in scientific investigations. It has a core knowledge base and a broad application. In a broad sense it means science done computationally. In a more focused sense, it means science of computing. Computational science mixes together several fields including computer science, applied mathematics and application sciences (such as earth sciences, chemistry, physics, biology, engineering, business among many others).

CS is not computer science which focuses on writing software programs and / or the development of new hardware products. CS is often defined as being that science which is at the intersection of science, computer science and mathematics. Alternatively known as modeling. Computational science looks to create and use computer models as a method of making observations, conducting experiments and creating or testing new theories. It is an interdisciplinary field that uses the technology of the computer to study problems in earth sciences, physics, chemistry, biology, mathematics and engineering fields. In computational science, the scientific problem must be expressed mathematically known as the algorithm. In this research an attempt has been made to produce the seismic energy map of Ethiopia by writing a FORTRAN code which computes seismic energy using the concept of sliding block analysis where the block is shifted by 0.5^0 either in latitude or longitude at a time then the total energy released within a 0.5^0 by 0.5^0 window for the whole period 2000 - 2002 is mapped to the center of the block.

1.1 Background Information

The East African Rift System (EARS) is a prominent feature on the African continent. Many of its characteristics like seismicity, volcanism, geothermal potential have been the subject of numerous studies. Seismicity is one of the many characteristics of the rift that continually draws interest to the region. An understanding of the seismicity of a region helps in quantifying risks posed by earthquakes, the stage in the evolution from a continental to an oceanic lithosphere and in understanding the structure beneath the rift. Magnitude and frequency of earthquakes occurring in the region is an indication of the accumulated stress and the stage in the rifting process thus a study of earthquake magnitude provides vital information.

b-value in the frequency - magnitude relation, $\log N = a - b \times M$, where N is the cumulative number of earthquakes having magnitudes equal to or greater than M and a, b are real constants that may vary in space and time which indicates stress accumulation levels in the region. Finally, a study of spatial distribution of seismic energy release (Es),

$\log Es = 4.92 + 1.55 \times M_b$, where M_b body wave magnitude, is one of the important means of gaining some insight into the evolution of seismicity in space (Ayele and Kulhánek. 1997 [9]).

1.2 Study Area

The main Ethiopian rift (MER) is part of the East African Rift system (EARS) and comprise of rift zones extending over a distance of 1000 km from Afar triangle junction at the Red Sea Gulf of Aden to the Kenya rift (Fig 1.1).

The main Ethiopian Rift system strikes NNE from its southern extreme (at 40.45^0) at lake Chamo (which is among Ethiopian Rift valley lakes) and continues 650 km until it reaches Ayellu volcano (at 90.45^0) and change its orientation from NNE with out any for discontinuity (Mohor,1967 [43]).

The west Ethiopian plateau is one part of Nubian plate (main African plate) that is located in the Eastern side of it and situated west of the east African rift system demarcated by elongated fault lines.

The east Ethiopian plateau is found between the main Ethiopian rift and the Somalia low land, being separated from the rift by sharp fault lines extended to its northern end. The MER is also the northern most segment of the Cenozoic East African rift system and connects with the Gulf of Aden and Red sea rifts within the Afar Depression to form a ride-ridge triple junction.

1.3 Geologic and Tectonic Setting

The East African Rift System (EARS) is generally considered to be a classic example of a continental rift. The Afar and Ethiopian portions of the rift system comprise the northern 1000 km of the EARS. This rift transects the broad Ethiopian plateau, which developed above a Paleogene mantle plume (Schilling, 1992. [49], Fig 1.2).

Recent studies in the Red Sea and Gulf of Aden show that flood basalts were erupted across a 1000 km diameter region at 30 Ma prior to or concurrent with the initiation of rifting (Menzies et al., 1992 [42]). There is little evidence for extension in the Afar/Ethiopian rift, the third arm of the triple junction, until considerably later (at $\sim$ 18 Ma; Wolde Gabriel et al., 1990 [52]). Since then the Main Ethiopian Rift has linked northwards into southern Afar and into oceanic spreading in the southern Red Sea (Makris and Ginzburg, 1987). Many of younger rifts in the EARS follow Precambrian and Paleozoic zones. Structural trends, however, the peak of rifting in Africa took place in the Cenozoic era and continued extending into late tertiary and recent times (Ghebreab, 1998 [26]). The EARS extends 3000 km from Afar depression in the north to Okavango Delta in the south through Djibouti, Ethiopia, Kenya, Uganda, Burundi, Rwanda, Democratic Republic of Congo, Tanzania, Zambia, Malawi, Zimbabwe and Botswana (Yirgu et al., 2006 [54]).

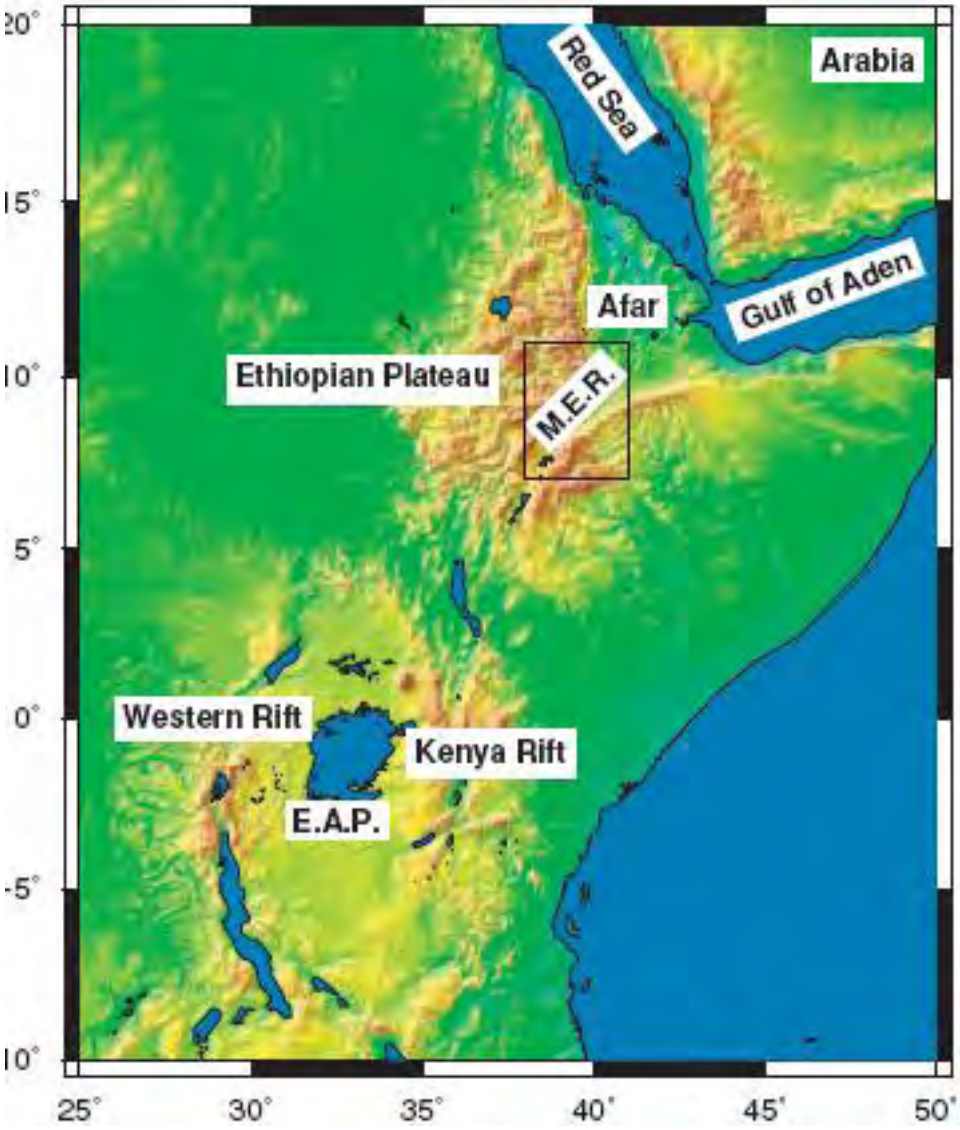

Figure 1.1: Regional map of the East African Rift system, Main Ethiopian Rift, E.A.P East African Plateau (Mackenzie et al., 2004)

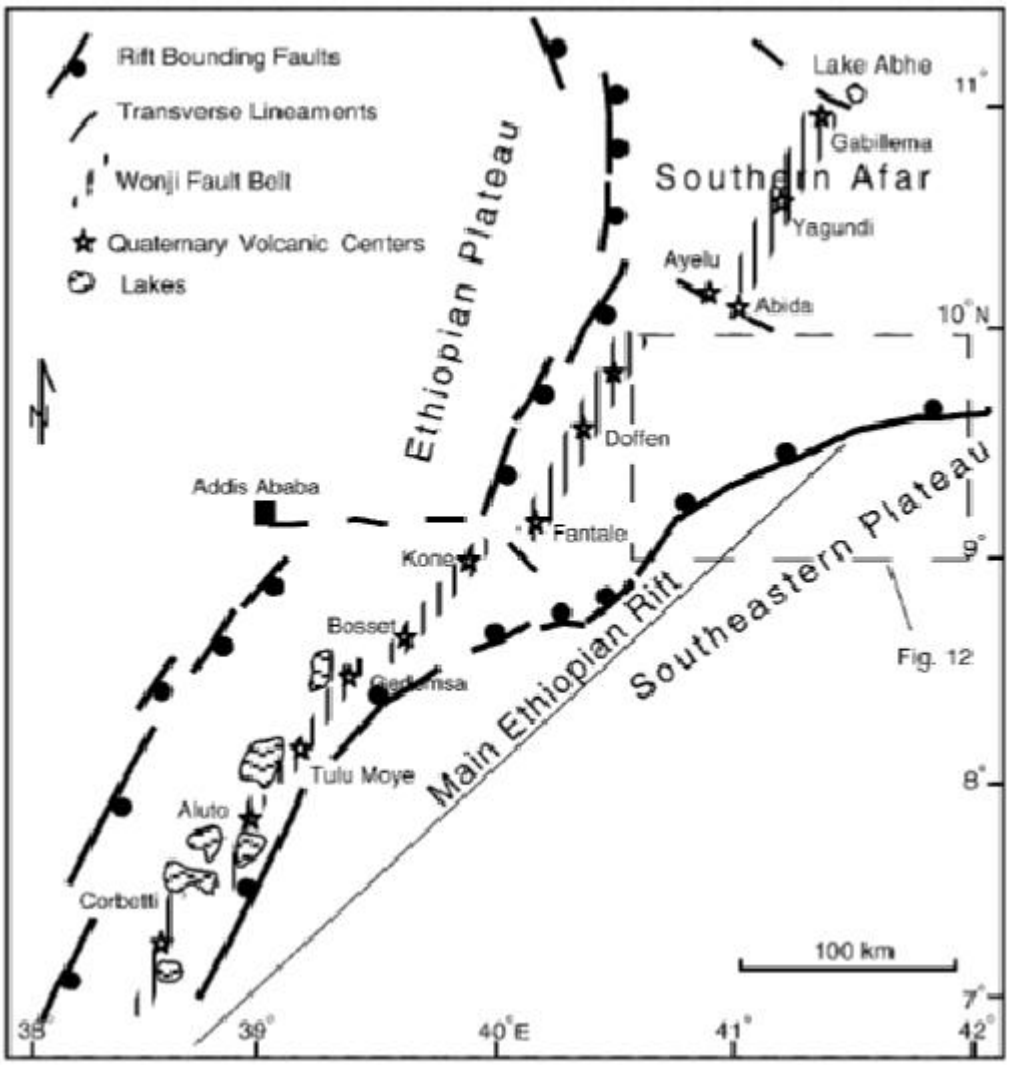

Figure 1.2: Tectonic outlines of the Main Ethiopian Rift and the Southern Afar Rift. The right-stepping Wonji Fault Belt and associated volcanic centers occupy the axial zone of the rift (Korme et al., 2003).

The EARS is also characterized by thinning of the lithosphere and propagation of low density material which gives rise to a negative Bouguer anomaly which extends from the junction of the Red Sea and Gulf of Aden through East Africa and then towards south west Africa at about 12^0 (Nolet, G., and Muller, S, 1982 [45]).

The NNE - SSW trending MER transects the uplifted Ethiopian plateau, which is believed to have developed in response to the impact of a Palaeogene mantle plume head on the base of the lithosphere (Schilling et al., 1992 [48]). This plateau is covered by extensive flood basalts that have been dated at 31 - 29 Ma (Hofmann et al., 1997 [30]) almost co-eval with opening of the Red Sea and Gulf of Aden rifts by c.30 and 28 Ma, respectively (Wolfenden et al., 2004 [53]). Rifting within the southern and central MER is believed to have occurred later, between 18 - 15 Ma (WoldeGabriel et al., 1990 [52]) and in the northern MER at c.11 Ma with formation of the Arboye border fault (Wolfenden et al., 2004 [53]). To the north, within the structurally complex Afar depression, the MER intersects the Gulf of Aden and the Red Sea rifts to form a tripe junction between the Nubian, Arabian and Somalian plates.

A change from 130^0 E- directed extension to 105^0 E- directed extension in the interval from 6.6 to 3 Ma is revealed by structural patterns (Boccaletti et al., 1998 [17]). Chu and Gordon (1999) [19] estimated the Nubian - Somalian separation since 3.2 Ma ago to be $>$ 5mm/yr across the northern MER and $\sim$ 16 mm/yr between Africa and Arabia across the Afar Depression. Bilham et al., (1999) [16] from geodetic measurements obtained for the NNE - trending MER an opening rate of 4.5 ± 1.0 mm/yr and extension direction of 108^0 E $\pm$ 10^0. The elliptical shape of the active volcanoes of Fantale, Boset and Dofen which have their major axis in the direction of plate motion led Ebinger and Casey (2001) and Casey et al. (2006) [21] to infer Holocene rift extension direction of N105^0 E. In contrast, Acocela and Korme (2002) [1], from field analysis of extensional fractures along the axis of the MER, determined a mean Holcene extension direction of N 52^0 W $\pm$ 20. This perpendicular extension direction to the MER, although, oblique to the active fractures

in the rift, was considered in their work as an indication of the kinematics between the Nubian and Somalian plates in Ethiopia.

The main Ethiopian Rift system strikes NNE from its southern extreme (at 40.45^0) at lake Chamo (which is among Ethiopian Rift valley lakes) and continues so for 650 km until it reaches Ayellu volcano (at 90.45^0) and change its orientation to NNW without any discontinuity. (Mohor 1967 [43]).

The map of earthquake epicenters in East Africa shows that the western branch of the rift is considerably more active than the central eastern branch (Fig 1.3, Fairhead & Girdler,1971; Nusbaum et al., 1993 [2]). Strong seismic activity runs from lake Mobutu in the north to Lake Malawi in the south, also a large area to the west of the rift is seismically active (Fairhead and Henderson, 1977; Foster et al., 1995 [2]).

1.4 Previous Seismotectonic Studies

It is expected that seismic activity associated with the rift development has been there for longer time in Ethiopia than the instrumentally and historically recorded data. The lack of earthquake recording instruments in the early days of earthquake occurrence and sparse distribution afterwards made the earthquake catalogue for the region incomplete. Records of seismicity over the past $\sim$ 150 years show seismicity concentrated near Ankober and within the en echelon magmatic segements along the axis of the MER (e.g., Gouin, 1979 [27]; Kebede and Kulhánek ,1994 [35]; Ayele and Kulhánek, 1997[9]).

Documented observations about the historic earthquakes for over 500 years in Ethiopia were collected from various sources and compiled by Gouin (1979) [27]. The distribution of these events shows that the Afar Depression and the western margin of the northern Ethiopian rift have a long history of seismic activity. In the monograph of Gouin (1979) the maximum magnitude of events observed in the whole region considered is 6.8. Some of the largest events are discussed in brief below. The August 25, 1906 earthquake with

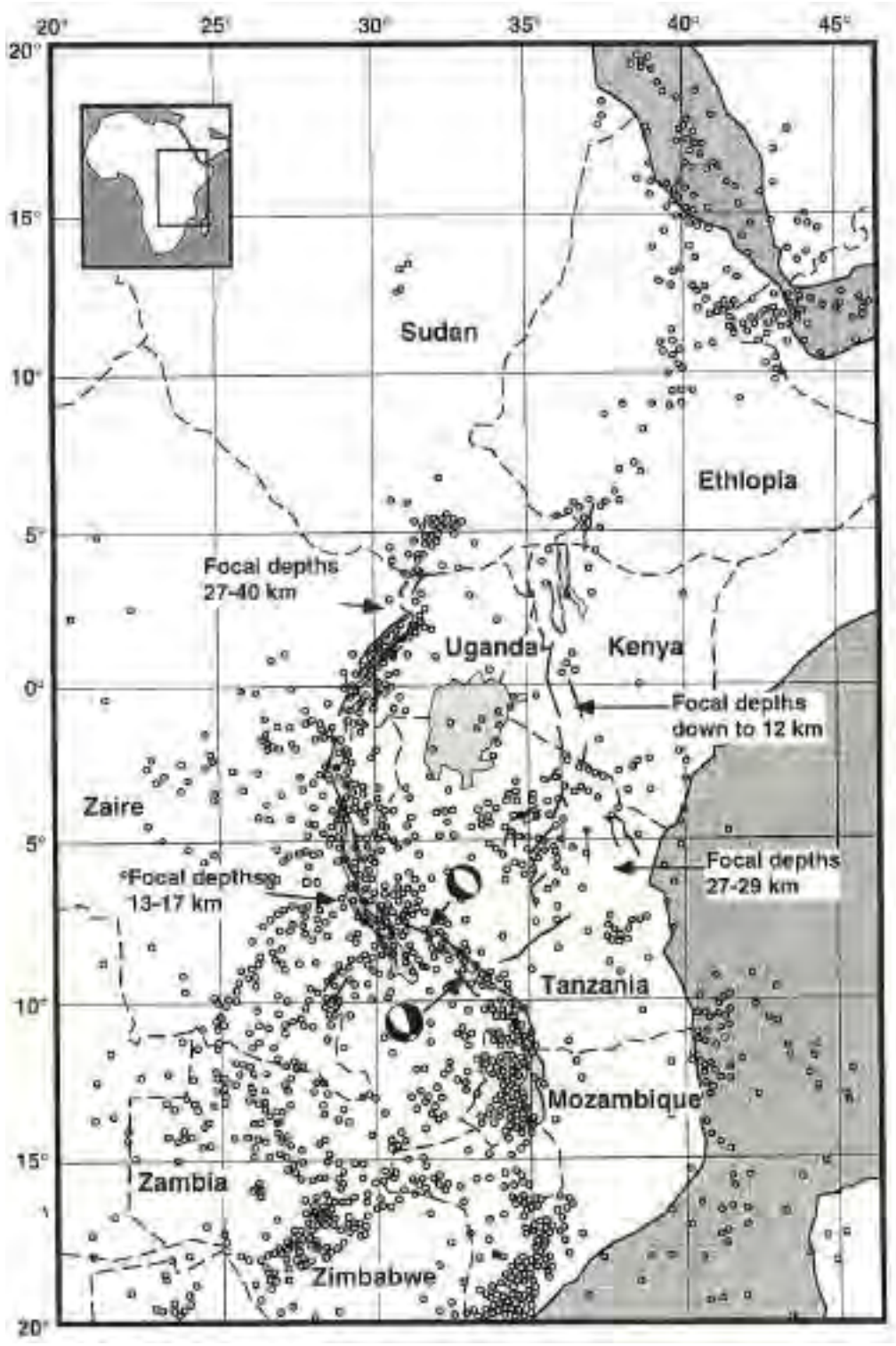

Figure 1.3: Map of the seismicity of East Africa from events recorded this century (Mostly from Nusbaum et al., 1993; fault plane solutions from Foster et al., 1995).

magnitude 6.8 (M_l) in the Langano area, which was also felt in Addis Ababa and its surroundings, is one of the reported events. This event is relocated by Ayele and Kulhánek (2000 [8]) to the eastern shoulder of the Ethiopian rift with M_w=6.6. An earthquake swarm was also reported in 1961 near Kara Kore which caused damage to manmade structures (completely destroyed the town of Majete) and alterations in the landscape the maximum magnitude was greater than 6.4. The other major event in the report is the May - March 1969 Serdo (in the central Afar Depression) earthquake sequence. The main shock had a magnitude M_b=5.9 that destroyed completely the town of Serdo with some causalities.

Earthquake catalogue of the Horn of Africa is also compiled for the period from 1960 - 1993 with a threshold magnitude of 4.5 (M_b) by Ayele (1995) [5]. This catalogue shows relatively high seismicity, considering the Ethiopian part only, in the Afar Depression and northern part of the western rift margin. In agreement with the localization of deformation to the magmatic segments (Bilham et al., 1999 [16]; Ebinger and Casey, 2001 [21]; Hofstetter and beyth, 2003 [31]; Wolfenden et al., 2004 [53]), the epicentral distribution for the MER for the period from October 2001 to January 2003 (Keir et al., (2006a) [36]) shows coincidence with these active centers. The only exception was the seismicity observed along the Ankober border fault. An increase in focal depth is observed as one goes from north to south along the rift system. These focal depth variation together with the low stress drop obtained for the Afar region was taken to infer the presence of soft material at a shallower depth in Afar and neighboring regions (Kebede, 1989 [33]). As an integral part of the seismicity study of the EARS and its parts, researchers have determined different b values. Kebede and Kulhánek (1991 and 1994 [35]) determined b-values of 0.5 - 0.8 for the Afar Depression and neighboring regions. The estimates of b-values obtained using information in (Ayele, 1995 [5]) are in the range from 0.5 to 1.1 for the north eastern part of the Ethiopian rift. Lower b-values are for the continental parts (Ayele and Kulhánek, 1997). This result is in agreement with the b-value of 0.67±0.16

calculated for the August 2002 swarm (Ayele et al., 2007 [11]). Keir et al ., (2006a)[36] using data from EAGLE estimated a b-value of 0.83±0.08 from 16 earthquakes obtained from global and regional catalogues that were located over a wide region in MER and southern Ethiopia.

According to Belachew (2007)[15], he obtained b-values of 1.059 ± 0.13 which could be taken as an indication that seismic energy was released in the region during the study period mainly in the form of small magnitude earthquakes. Brazier et al, 2006 [48] also estimated b value of 1.25 on the study of local magnitude scale for the Ethiopian Plateau.

1.5 Statement of the problem

Seismicity is one of the many characteristics of the rift that continually draws interest to a region. An understanding of the seismicity of a region helps in quantifying seismic risks. The magnitude and frequency of earthquake occurring in the region is an indication of the accumulated stress and the stage in the rifting process. Seismic energy mapping is one of the important means of gaining some insight into the evolution of seismicity in space (Ayele and Kulhánek, 1997)[9]. The seismic energy mapping of the study area has not been conducted for the time period (2000 - 2002). The study asses seismic energy mapping by developing Fortran code, computer programming approach.

1.6 Objectives and Significance of the Study

This paper asses the seismicity of MER and Afar for the period between 2000 and 2002. Brazer et al., 2006 [48] and Belachew,2007 [15] studied on the same area and time period. However, when we compare the seismicity map of MER and Afar produced by Brazer et al., 2006 with other related maps on the given area, Brazer's map is more scattered and some of the distribution of the earthquakes is not on the expected locations as close to the rift which was the motivation for this work.

The following are considered to be the primary aims of this paper: Revisiting Braizer et al., 2006 scattered locations of events by

1. *Developing an earthquake catalogue of Afar and main Ethiopian rift for the period 2000 - 2002*
2. *Estimating the b-value and interpreting the result*
3. *Developing seismic energy map for the whole region for the time period specified*

Chapter 2 review some of the important background of seismic theory followed by an overview of the data sources which are available for use in this study. The study will then proceed with Methods, Results and Discussions and conclusions in chapters 4,5 and 6 respectively.

CHAPTER 2

Theory

2.1 Seismic Wave Propagation

Earthquakes are generated as result of transient stress imbalances in the interior of the earth. During an earthquake seismic (elastic) waves are generated. Seismology studies the origin (source nature) of the waves their propagation through the earth's interior and their recording and interpretation by analyzing ground motions recorded at some distance from the source. Earthquake sources are either natural such as earthquakes faulting or manmade cause like underground nuclear bomb explosions. The distribution of earthquakes shows us where the earth is active and the passage of seismic waves through the earth allows us, as it were to CAT- scan its interior (Fowler, 1995 [24]). When an earthquake or an explosion occurs within the earth, part of the energy released takes the form of elastic waves which are transmitted through the earth. These waves can be detected by instruments called seismometers, which measure, amplify and record (on paper,magnetic tape or disc) the motion of the ground on which they are positioned. The speed with which these elastic waves travel depends on the density (ρ) and elastic moduli (μ) of the rocks through which the waves pass. There are two types of elastic waves: a) Body waves and b) Surface waves

a. Body waves - are seismic waves which travel through the body of the earth. Body waves are reflected and transmitted at interfaces where the seismic velocity and /or density change, and they obey Snell's Law.

There are two types of body waves:

1. P- waves (P stands for primary or pressure or push pull). These waves involve compression and rarefaction of the material as the wave passes through it but not rotation. P-waves are most correctly called dilatational or irrotational waves. They are the analogue in a solid of sound waves in air.

2. S- waves (stands for secondary). These waves involve shearing and rotation of the materials as the wave passes through it but not volume change. S - waves are most correctly called rotational waves. The P - wave particle motion is longitudinal, meaning that particles making up the medium through which the P - wave is passing vibrate about an equilibrium position in the same direction as the direction in which P - wave is traveling. In contrast, the particle motion of S- waves is transverse that is perpendicular to the direction of the S - wave. The S - wave motion can be split in to a horizontally polarized motion termed SH and a vertically polarized motion termed SV.

b. Surface waves: Surface waves (Love and Rayleigh waves) on the other hand, propagate only along the surface of earth. Love waves (name after A.E.H.Love (1863 - 1940)) have a particle motion at right angle to the direction of propagation, Rayleigh waves (name after Lord Rayleigh (1842 - 1919) have a retrograde particle motion, meaning that the particle motion is circular, opposite the direction of propagation.

When there is a stress imbalance, deformation or strain result, which in turn generates seismic waves. Therefore, the key problem in seismology is the study of the relation between the deforming forces in a medium and the resulting deformation. To fully describe and interpret a seismic record which is the result of the combined effects of the source, propagation path and recording instrument, understanding of the basics of wave propagation theory is necessary. In the following sub - sections the basic theories are discussed briefly.

2.2 The Theory of Elasticity

An earthquake occurs in the earth's interior (crust and upper mantle) when the tectonic stress (deformational force applied per unit area) exceeds the local strength of the rocks and failure occurs. The resulting seismic elastic waves propagated away from the source region by elastic deformation of the rocks through which they travel. Therefore, their propagation depends on the elastic properties. The theory of elasticity provides mathematical relationships between the forces applied on a medium stresses and the resulting deformations strains. The relation between stress and strain is used to describe the elastic properties of a medium. It is given by the generalized form of Hook's law as :

$$\sigma_{ij} = c_{ijkl} \times \varepsilon_{kl} \tag{2.2.1}$$

where σ_{ij} is the stress tensor, c_{ijkl} represent the constants of proportionality known as elastic moduli and ε_{kl} is the strain tensor.

2.3 Stress and Strain Tensors

Stress is defined as force per unit area. If the force is perpendicular to the area, the stress is said to be normal stress or pressure and when it is parallel to the area element, it is called shear stress. Usually the force is neither entirely normal nor tangential but is at some arbitrary intermediate angle in which case it can be resolved into components which are normal and tangential to the surface. The sign of convention is that tensional stress are positive and compressional stresses are negative. For the purpose of the theoretical modeling, let's consider infinitesimal cubic element of volume inside a continuum bounded by faces paralleling the coordinate planes, the stresses acting upon each of the six faces of the element can be resolved into components as shown in Fig 2.1.

When the medium is in static equilibrium, the stress must be balanced i.e, the three stresses σ_{11}, σ_{12} and σ_{13} acting on the front face must be equal and opposite to the corresponding stresses on the opposite face with similar relation for the remaining four

faces that is,

$$\sigma_{ij} = \sigma_{ji} \tag{2.3.1}$$

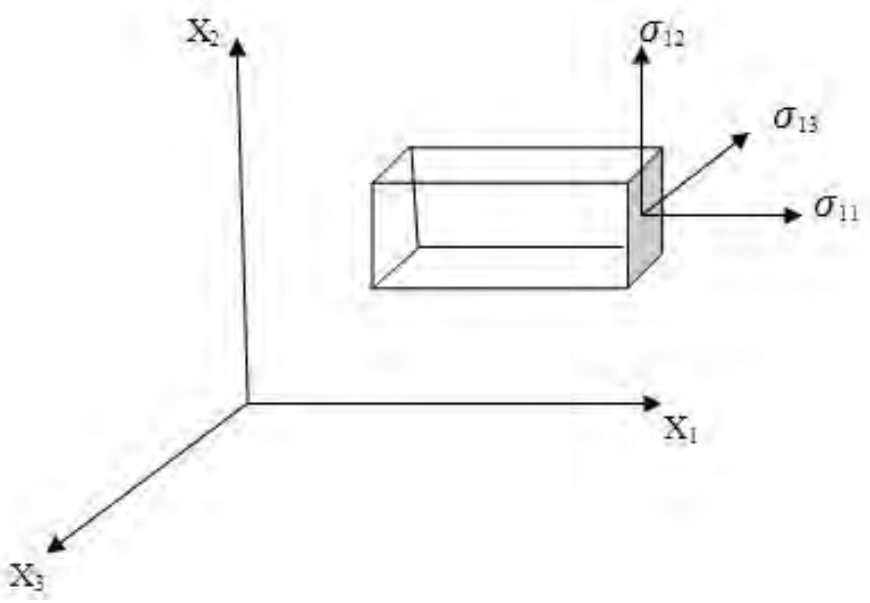

Figure 2.1: A cubic element in a continuum. Balancing the stresses on each face acting in a given direction leads to the equation of equilibrium only the stresses on $+X_1$ faces are shown, similar stress component exist on each face.

The total stresses are σ_{11}, σ_{22} and σ_{33} which are normal stresses and σ_{12}, σ_{13}, σ_{21}, σ_{23}, σ_{31} and σ_{32} which are shear stresses. Therefore, mathmatically the total stress can be described by 2^{nd} rank Tensor as:

$$\sigma = \begin{pmatrix} \sigma_{11} & \sigma_{12} & \sigma_{13} \\ \sigma_{21} & \sigma_{22} & \sigma_{23} \\ \sigma_{31} & \sigma_{32} & \sigma_{33} \end{pmatrix} \tag{2.3.2}$$

2.3.1 Strain Tensor

When an elastic body is subjected to stresses, changes in shape and dimensions occur. Strain is defined as the relative change in a dimension or shape of a body. By similar argument just like the derivation of stress above, the relation between the strain and fractional change in dimension can be done (Aki and Richard, 1980)[4]. For three displacements (u_1,u_2,u_3), which represent dimensions of a material element that change as a result of applied stress, the strains are thus divided as those that involve length changes (normal strain) and those involve angular distortions (shear strains).

The normal strains are given as:

$$\varepsilon_{11} = \frac{\partial u_1}{\partial x_1} \tag{2.3.3}$$

$$\varepsilon_{22} = \frac{\partial u_2}{\partial x_2} \tag{2.3.4}$$

$$\varepsilon_{33} = \frac{\partial u_3}{\partial x_3} \tag{2.3.5}$$

And the shear components as:

$$\varepsilon_{12} = \frac{\partial u_2}{\partial x_1} + \frac{\partial u_1}{\partial x_2} = \varepsilon_{21} \tag{2.3.6}$$

$$\varepsilon_{23} = \frac{\partial u_3}{\partial x_2} + \frac{\partial u_2}{\partial x_3} = \varepsilon_{32} \tag{2.3.7}$$

$$\varepsilon_{31} = \frac{\partial u_1}{\partial x_3} + \frac{\partial u_3}{\partial x_1} = \varepsilon_{13} \tag{2.3.8}$$

Hence the strains can be described by 2^{nd} rank tensor as:

$$\varepsilon = \begin{pmatrix} \varepsilon_{11} & \varepsilon_{12} & \varepsilon_{13} \\ \varepsilon_{21} & \varepsilon_{22} & \varepsilon_{23} \\ \varepsilon_{31} & \varepsilon_{32} & \varepsilon_{33} \end{pmatrix} \tag{2.3.9}$$

In compact indicial notation the shear strains can be represented as:

$$\varepsilon_{ij} = \frac{1}{2} \times (u_{ij} + u_{ji}) \tag{2.3.10}$$

The C_{ijkl} term in Eq (2.2.1) has 81 terms for the general form relating the nine elements of the stress tensor. Applying the symmetric natures of the stress and strain tensors and further assuming homogenous, isotropic and linearly elastic medium the number of elastic constants can be reduced to only two. These constants are known as the Lame constants, λ and μ and they are related to c_{ijkl} by:

$$c_{ijkl} = \lambda\delta_{ij}\delta_{kl} + \mu(\delta_{ik}\delta_{ji} + \delta_{il}\delta_{jk}) \tag{2.3.11}$$

where δ is the kronecker delta function. Substituting Eq (2.3.11) in to Eq (2.3.1) gives

$$\sigma_{ij} = [\lambda\delta_{ij}\delta_{kl} + \mu(\delta_{ik}\delta_{ji} + \delta_{il}\delta_{jk})]\varepsilon_{kl} \tag{2.3.12}$$

This reduces to:

$$\sigma_{ij} = \lambda\theta\delta_{ij} + 2\mu\varepsilon_{ij} \tag{2.3.13}$$

where $\theta = \dfrac{\partial u_1}{\partial x_1} + \dfrac{\partial u_2}{\partial x_2} + \dfrac{\partial u_3}{\partial x_3}$

δ_{ij} is the kronecker delta function and is given by $\delta_{ij} = 1$ for $i = j$ and $\delta_{ij} = 0$ for $i \neq j$.

2.4 Equation of Motion

The propagation of the elastic disturbances which resulted from the stress imbalance in a medium can be mathematically represented using the above equations of stress, strain and the generalized form of Hook's law. Taking into account the effects of body forces in a medium and applying Newton's 2^{nd} law, the equation of motion is given by the general

formula as:

$$\rho\frac{\partial^2 u_i}{\partial t^2} = f_i + \frac{\partial \sigma_{ij}}{\partial x_i} \tag{2.4.1}$$

where ρ is density of the material and f_i is the body force per unit volume. Since the body forces such as gravitational forces do not vary much with distances (Aki and Richards ,1980)[4], the homogenous equation of motion is given by neglecting the body force terms from Eq (2.4.1) as

$$\rho\frac{\partial^2 u_i}{\partial t^2} = \frac{\partial \sigma_{ij}}{\partial x_i} \tag{2.4.2}$$

Substituting Eq (2.3.10) and Eq (2.3.13) into Eq (2.4.2), we can write the three dimensional vector equation of motion for a homogeneous, isotropic, linear elastic medium as

$$\rho\frac{\partial^2 u_i}{\partial t^2} = (\lambda+\mu)\vec{\nabla}(\vec{\nabla}.\vec{u}) + \mu\vec{\nabla}^2 u \tag{2.4.3}$$

where ∇ is the del operator and ∇^2 is the Laplacian operator. Using the vector identity

$$\vec{\nabla}^2 u = (\vec{\nabla}.\vec{u}) - (\vec{\nabla}\times\vec{\nabla}\times\vec{u}) \tag{2.4.4}$$

Eq (2.4.3) can be rewritten as

$$\rho\frac{\partial^2 u_i}{\partial t^2} = (\lambda+2\mu)\vec{\nabla}(\vec{\nabla}.\vec{u}) - \mu(\vec{\nabla}\times\vec{\nabla}\times\vec{u}) \tag{2.4.5}$$

Eq (2.4.3) and (2.4.5) are of the form, Force=mass$\times$ acceleration, in terms of particle displacements for a general deformation transmitted through a homogeneous, isotropic, linearly elastic medium, the equations are based mainly on the assumptions of infinitesimal strain and no body forces.

2.5 Earthquake Magnitude

Earthquake magnitude is a measure of the energy released during the earthquake. It is determined from the logarithm of the maximum amplitude of the earthquake signal as seen on the seismogram with a correction for the distance between the focus and the seismometer. Several different magnitude scales exist based on the different types of seismic wave.

The Richter local magnitude (M_l) is defined to be used for local earthquakes up to 600 km away and is calculated using high - frequency data from nearby stations. Surface wave magnitude (M_s) is based on the maximum amplitude of the surface waves and body wave magnitude (M_b) is calculated from body waves. Although these magnitudes can be calculated at any epicentral distance, M_s is usually used for observations near the earthquake epicenter where the surface wave is larger than the body wave and M_b is usually used at larger distance from the epicenter (amplitude attenuation of body waves is less than that of surface waves). Moment magnitude (M_w) is considered the most reliable measure of earthquake size, especially for largest events since M_s is saturates at about magnitude 8. It is calculated by analysis of the frequency spectra of the earthquake. Note that since all magnitude scales are logarithmic, an increase of 1 magnitude point represents a 10 - fold increase in ground motion and a 30 - fold increase in energy released. Earthquake Intensity describes the degree of shaking caused by an earthquake at a given place and decreases with distance from the earthquake epicenter. Whilst magnitude measurement requires instrumental monitoring for its calculation, intensity can assigned based on testimony of the population. Several scales exist; the Modified Mercalli scale is commonly used in the US.

2.6 b-Values of Earthquake Sequence

Seismologists have long recognized that the frequency of earthquake occurrence tends to follow a power law with respect to size. Define N to be the number of earthquakes per year above a certain magnitude M_l.

The power law for an earthquake occurrence takes the form of :

$$\log N = a - b \times M_l \tag{2.6.1}$$

both parameters a and b are determined empirically by a statistical fit to data in seismicity catalogs. The relative frequency of large and small earthquakes is described by the parameter b, sometimes called the b-value. The parameter a, describe the activity

of a seismogenic region. For world wide seismicity, a is roughly 8 and b=1 to a good approximation. Using these values, one can predict N=100 earthquakes per year world wide with Richter magnitude $M > 7.0$. As b-value increases, large earthquakes become less numerous, and fault motion at plate boundaries becomes smoother, with fewer large jumps. As the b-value decreases, larger earthquakes become relatively more numerous, and fault motion becomes rougher.

2.7 Seismic Energy

Seismic energy is defined as the energy released during an earthquake. It is also possible to relate magnitude of an earthquake to the seismic energy released. As noted above, the magnitude scales measures earthquake size in a relative manner. In other words, it compares large and small earthquakes quantitatively, but indicates little about the physical properties of other sources. For a more precise discussion of a seismic source property, therefore, we need to relate the scale a basic physical parameter such as energy (Kasahara,1981 [32]).

Seismic energy release (Es) can be calculated with the relation

$$LogEs = 1.55 \times M_b + 4.92 \tag{2.7.1}$$

where Es is in joules and M_b is body wave magnitude (Båth.1979 [13]).

CHAPTER 3

Data Acquisition and Processing

3.1 Data Sources

The data for this thesis is found from the IGSSA (Institute of Geophysics Space Science and Astronomy) of Addis Ababa University. The data is a high quality earthquake wave-form dataset recorded by Incorporated Research Institutes of Seismology /Program for the Array Seismic Studies of the Continental Lithosphere (IRIS/PASSCAL) Broadband Seismic Experiment recently conducted in Ethiopia (Nyblade and Langston ,et al ;2002) and Ethiopian Seismic Station Network (ESSN). This experiment was operational between 2000 and 2002. The 26 three component broadband seismic stations of this experiment were distributed in the country (Fig 3.1) covering an area of 500× 500 km^2. The data is in SEGY format.

3.2 Data Processing

3.2.1 Seismic phase Picking

The REFTAKE wave form data were converted in to SEGY and SAC wave format so that it is ready for plotting using PQL and SAC (Seismic Analysis Software). P- and S- first arrival times were picked from vertical and horizontal components, respectively (Fig 3.2). In cases where the noise level for the records is higher various filters were applied to determine the arrival times with better accuracy. Arrival times were read for all Earthquakes, regardless of their size and source region, recorded by the stations for year 2000 - 2002.

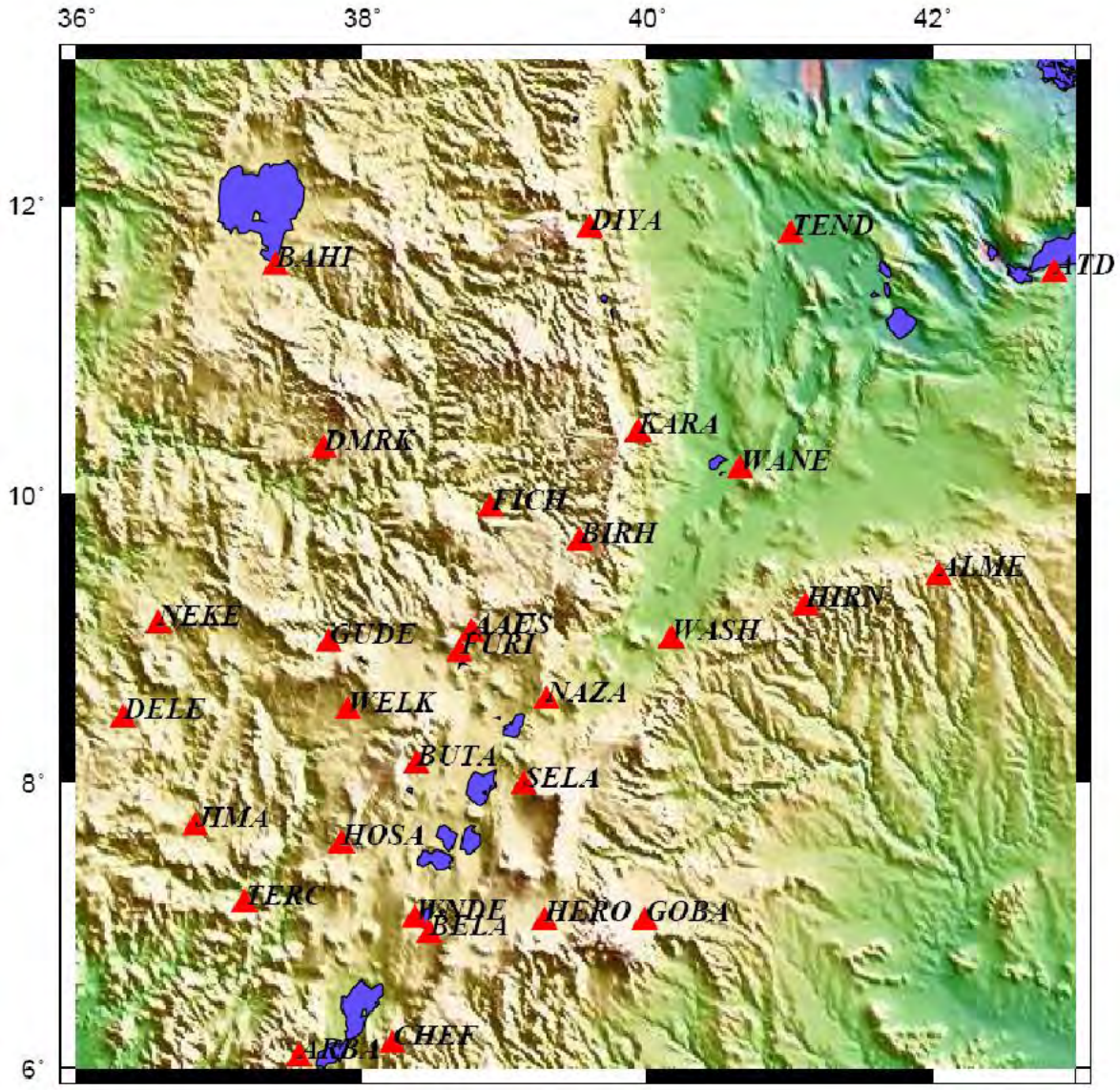

Figure 3.1: Distribution of earthquake recording stations used in this study. Red triangles mark the locations of the IRIS / PSSCAL experiment stations..

After the arrival time were picked the location of events was done by SEISAN (Seismic Analysis) software.

3.2.2 SEISAN Software

SEISAN software has numerous sub programs capable of among other things, locating earthquakes, plotting waveforms, doing earthquake statics and spectral analysis and determining earthquake focal mechanisms. These subprograms are run as stand alone programs or using the driver program EEV.

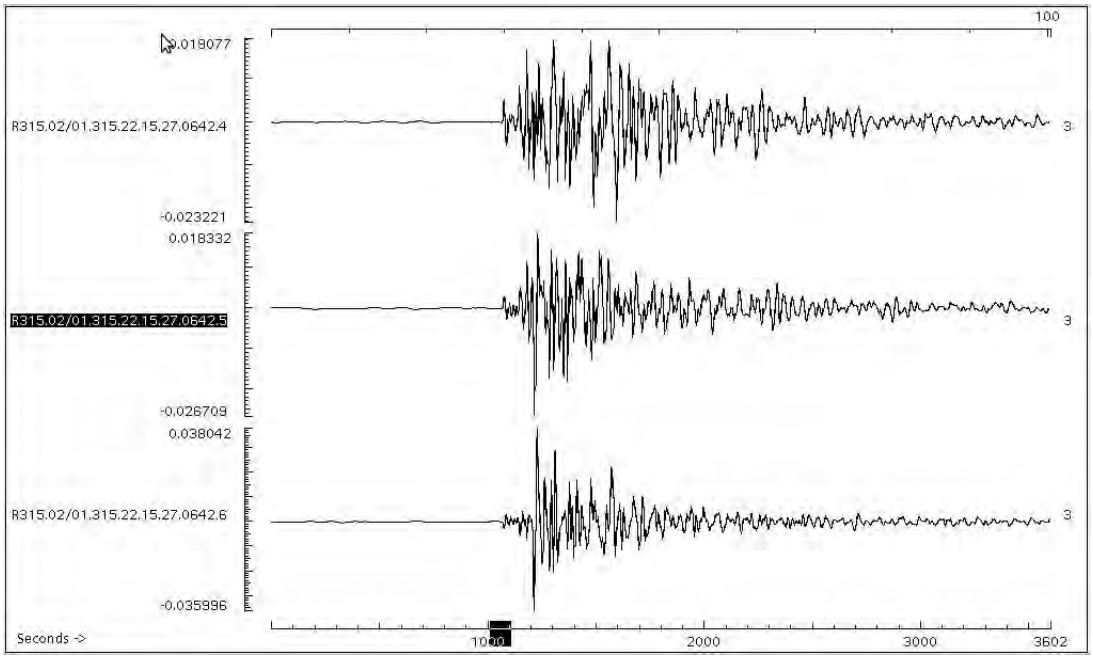

Figure 3.2: This is an example of a PQL format unfiltered wave form station Bahir Dar. It is from a Broadband instrument with the vertical component at the top followed by the North - South then East - West component respectively.

3.2.3 Event Location

The location program currently used for locating earthquakes is Hypocenter (Lienert et al.,1986) and it is achieved using the HYP sub program. To locate an event, HYP requires at least three different phases, i.e. P,S arrivals or their derivatives and azimuth. Once the

above requirement is met, location can be done for both single and multiple station data. Coda magnitude is also calculated for all events with P coda duration.

B-VALUE is the SEISAN subprogram for calculating b - value from the cumulative frequency - magnitude plot. It takes a Nordic file (Table 3.1) input, e.g. collect.out or select.out. When running the program one needs to specify the source file name, type of magnitude to be read in the calculation, magnitude range, magnitude step and a fixed b - value at which to calculate the value of a. The program produces an output file with all output parameters and a plot of the b value. In SEISAN software first a data base were created from single event files (S-files or catalogue files). To register events in the data base, firstly the collect.out files are split in to the database using a SEISAN subprogram called SPLIT, this program splits the S-files into the approximate month and year folders of the data base.

S-files

An S - file is a parameter fie in SEISAN (Nordic) format generated by the SEISAN sub program NEWEVE.

Table 3.1 shows S-file for an earthquake which occurred on 10 MAY 2001 at 16:50:05 GMT; at latitude 6.626^0 N and longitude 41.72^0 E. It was reported by stations KARA, ARBA, FICH and DMRK. At all the three stations, phases were picked from the vertical component of a short period seismometer. The picked phases are emergent P wave EP, emergent -S. Among others available data on this S-file include coda length, azimuth, angel of incidence (AIN), travel time residuals (TRES), distance (DIS) and name(s) of wave form file(s) generated for the earthquakes.

Data is analyzed by splitting the S - files for similar event, update has been made using the command UPDATE this program updated the S - files one or several months at a

2001 510 1650 5.4 L 6.662 41.721 2.0 AFA 4 1.2 2.9CAFA GAP=287 2.32 67.2 23.1 0.0 0.2702E+03 0.2782E+04 0.4052E+04E ACTION:UPD 11-04-03 16:10 OP:sisa STATUS: ID:20010510165038 L I STAT SP IPHASW D HRMM SECON CODA AMPLIT PERI AZIMU KARA SZ EP 1651 10.41 33 1.0210 460 335 ARBA SZ EP 1651 09.90 33 -0.0710 466 262 FICH SZ EP 1651 10.99 120 33 -1.9210 487 326

Table 3.1: S-file for an earthquake which occurred on 10 MAY 2001 at 16:50:05 GMT

time in order to ensure that nothing is forgotten with in a month. After location the database was checked for events with large RMS values, longitude, latitude, depth errors. The selection of such event was done using the program SELECT, while after a number selection criteria. All the above mentioned errors results from large travel time residuals i.e. large differences in observed and calculated travel times. These large residuals are due to poorly picked phases and when manually entering phase picks, verification of picked phases was done by plotting epicenters and error ellipse using the command J SEISAN. Errors due to wrong picked phases were corrected by re picking the phases. b - values were generated for the whole database using the sub program BVALUE. Data was selected from the data base using the subprogram SELECT by specifying the region of interest using latitude and longitude boundaries.

CHAPTER 4

Methodology

4.1 Energy Mapping

The geographical distribution of epicenters alone may not be enough to obtain a introductory picture of potential hazard areas. Epicentral clustering of each tremors can not easily expressed the size of seismic energy being released in a seismically active region. Energy mapping is one of the important means of gaining some insight into the evolution of seismicity in space (Ayele and Kulhánek, 1997 [9]).

Using data fro regression analysis shown below in the Fig 4.1, the body magnitude is converted in to coda magnitude by the relation :

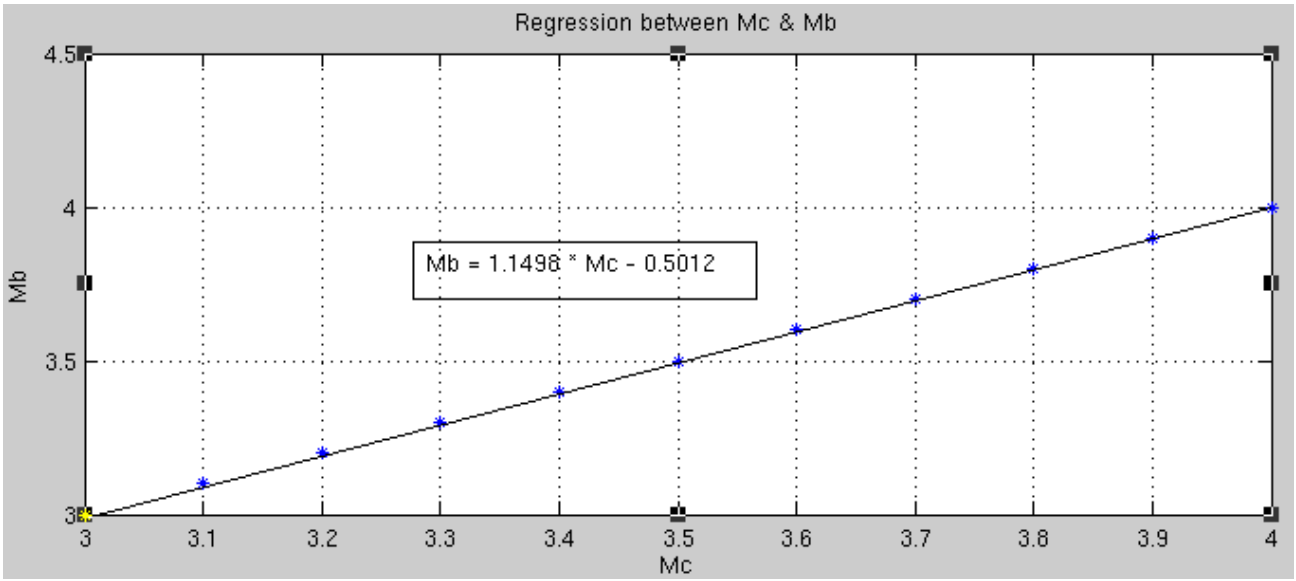

Figure 4.1: Regression relation between body magnitude (M_b) and coda magnitude (M_c).

$$Mb = 1.15 * Mc - 0.50 \tag{4.1.1}$$

Using Eq (4.1.1), Eq (2.7.1) becomes

$$\log Es = 1.78 * M_c + 4.15 \tag{4.1.2}$$

The energy is calculated using the concept of sliding block analysis where the block is shifted by 0.5^0 either in latitude or longitude at a time then the total energy released in Eq (4.1.2) is calculated within a $0.5^0 \times 0.5^0$ widow for the whole period and the computed value is mapped to the center of the block (Fig 5.4), this narrow window is chosen to minimize the space smoothing. Es is not statistically dependent on the number of samples unlike the b - value. The method used to map the seismic energy release is Fortran Program. See (APPENDIX B and C).

4.1.1 Estimation of b-values

The frequency magnitude distribution (FMD) or the earthquake recurrence relation describes the number of earthquakes occurring in a given region as a function of their magnitude M as in equation (2.6.1). This relation is usually referred to as the Gutenberg and Richter (G-R) [28] or frequency magnitude distribution. When plotting the cumulative number of earthquakes versus their magnitudes (FMD), b represents the slope of the best fitting line for a certain magnitude range and is inversely proportional to the average size of faults that rupture during earthquakes (Aki, 1965) [3]. Values of b are close to 1.0 in the Earths crust (Frolich and Davis, 1993) [25] but in volcanic regions b is commonly higher than 1.0 (Wiemer and McNutt, 1997) [51]. This anomalously high b-value at volcanoes has been accredited to excessive material heterogeneity (Mogi,1962). To calculate the b-value in Eq (2.6.1), we apply the method of linear least square regression or maximum - likelihood method of Aki (1965)[3].

According of this method the b-value is expressed as [1]

$$b = \frac{Log_{10}(e)}{(M_{av} - M_{min})} = \frac{0.43}{(M_{av} - M_{min})} \tag{4.1.3}$$

where $M_{av} = \sum_{i=1}^{n}(\frac{M_i}{N})$
is the mean magnitude, N is the number of events larger than M_{min} and M_{min} is the minimum magnitude (threshold magnitude) of the given sample. In most caseses the minimum magnitude which relies on the magnitude distribution in Eq (2.6.1) is determined by plotting the cumulative number of events as a function of magnitudes.
According to Shi and Bolt (1982) [49], the standard error (σ) of the maximum likelihood estimation of b is approximated by

$$\sigma(b) = 2.30 \times b^2 \times \sqrt{\frac{\sum_{i=1}^{n}(M_i - M_{av})^2}{n(n-1)}}$$

where M_i' s are the individual M_l values and n is the number of magnitude observations considered.

[1] data for regression analysis is from Chimlambe, 2008 [14]

CHAPTER 5

Results

In this chapter the results found in this thesis is presented. Coda magnitudes for 238 events have been estimated, see (Appendix A). These events are located by GMT software on Linux are shown below (Fig 5.1). Earthquake located with accuracy of an average RMS (root - mean - square) of 0.5 is the comparison of the estimated coda magnitude (M_c) with the magnitudes estimated by Braizer et al.,2006 [47].

Seismic activity during the study period was distributed all along the rift system with relatively high concentration around 9^0 N and 40.5^0 E; 9.5^0 N and 39.5^0 E - near Dofen volcano and Ankober border fault.

A b - value of 0.90 $\pm$ 0.09, above the threshold magnitude of 2.75, is estimated using the maximum likelihood method (Aki ,1965) [3] and an error estimate determined from the standard deviation of b (Shi and Bolt ,1982) [49]. Using the least square method the b - value found as 1.01 which is nearly comparable with the maximum likelihood method. The difference between the two results is due to the fact that least square method is disproportionately influenced by the largest earthquakes while the maximum likelihood weighs each earthquake equally which is close to true value of b. The cumulative frequency magnitude distribution of Ankober - Dofen earthquake sequence is drawn by SEISAN software as shown below (Fig.5.2) The slope of the graph shown below for local magnitudes in between 2.75 and 3.7 is 0.90 $\pm$ 0.09 using the maximum likelihood method (Aki, 1965)[3] and standard deviation of 0.09.

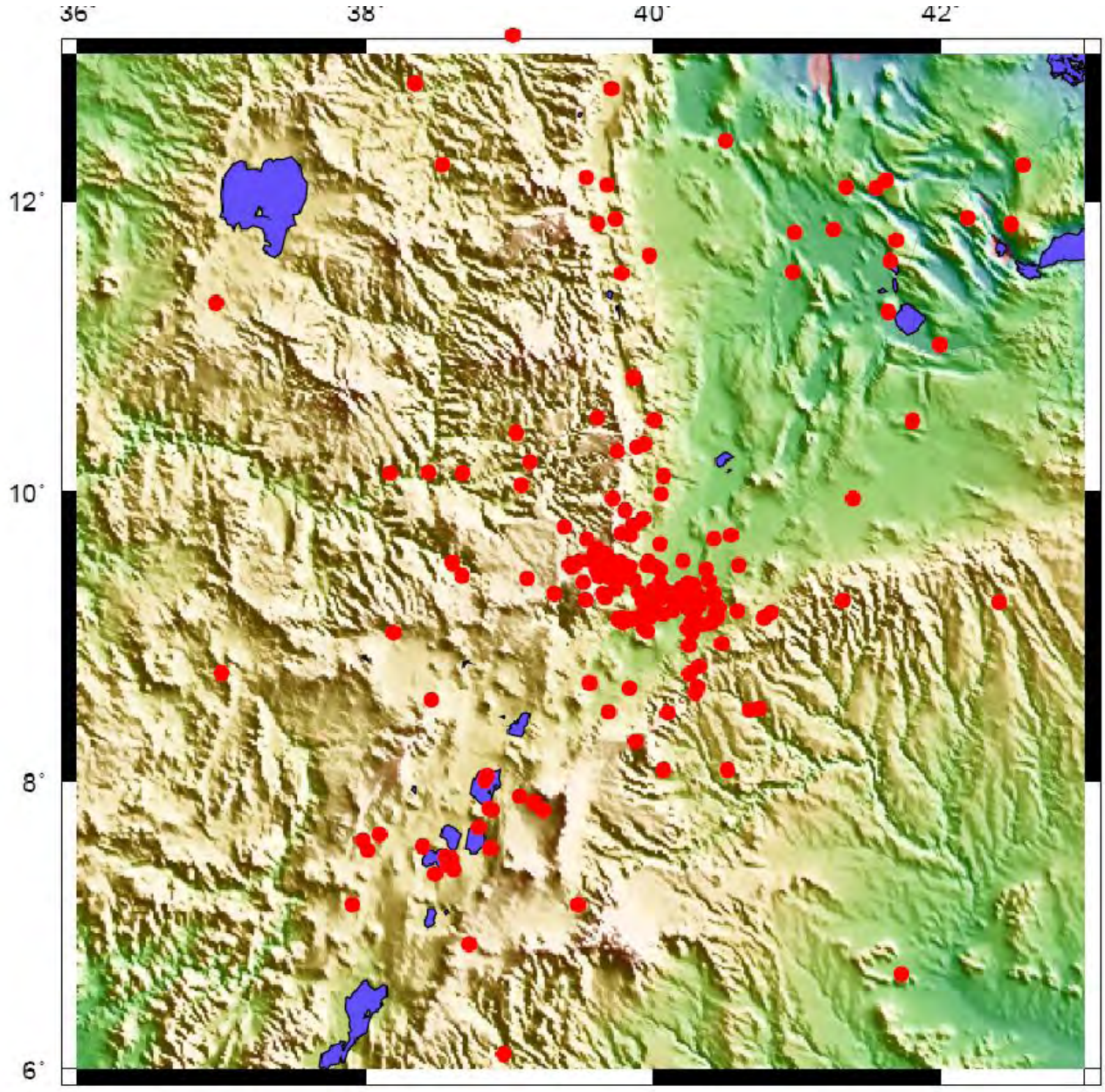

Figure 5.1: Locatioins of epicnenters determine for the period between 2000 and 2002. The red circles mark epicentral locatioins determined in this study

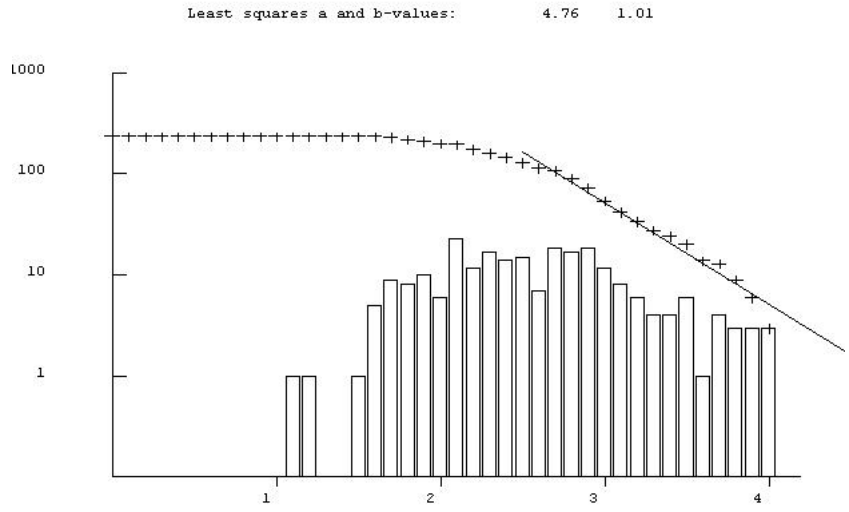

Figure 5.2: FMD plot for the whole area using least square method. The threshold magnitude, Mt=2.75 above which the catalogue is complete. The straight line is a least squares fit to the data above the threshold magnitude. The slope of the straight line is 1.01. The vertical axis represents the number of earthquakes (N) and the horizontal axsis represents the coda magnitudes of earthquakes (M_c).

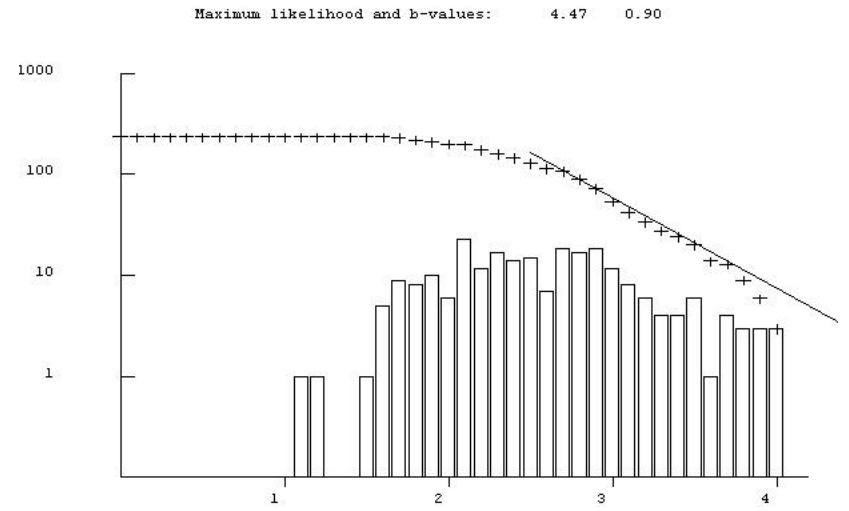

Figure 5.3: FMD plot for the whole area using Maximum likelihood method. The vertical axis represents the number of earthquakes (N) and the horizontal axsis represents the coda magnitudes of earthquakes (M_c).

The seismic energy map shown in Fig 5.5 is produced by the program that is written in this thesis using the data between 1960 - 1993, the result is exactly the same as produced by Ayele et al., 1997 [9] (Fig 5.4).

The seismic energy map of the study area also is produced and plotted as shown below (Fig.5.6).

Using the same program, Brazier et al.,2006 energy mapping is produce and it is shown below, Fig 5.7

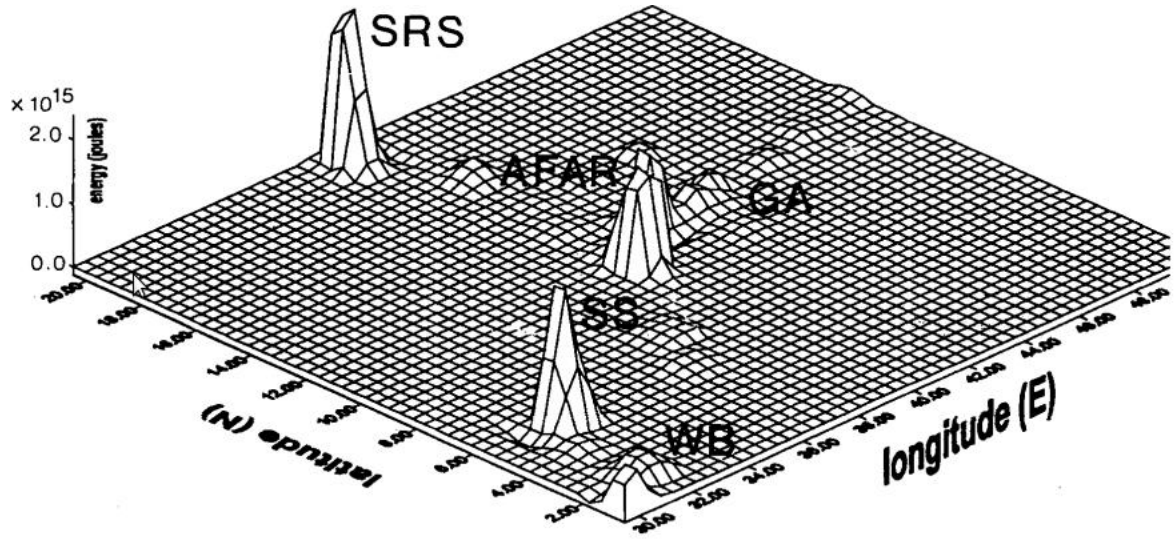

Figure 5.4: Spatial variation of seismic energy release for the period 1960 - 1993. Dominant energy peaks, up to 2 $\times 10^{15}$J, are observed in the Southern Red Sea (SRS), Afar and Southern Sudan (SS) (GA : Gulf of Aden; WB: Western Branch).(Ayele and Kulhanek ,1997)[9].

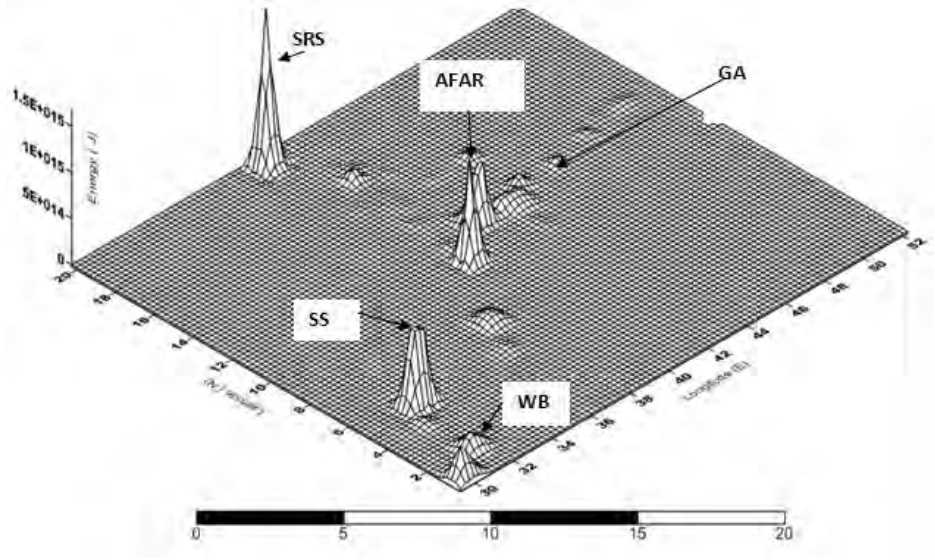

Figure 5.5: Spatial variation of seismic energy release for the period 1960 - 1993 using the program written in this study.

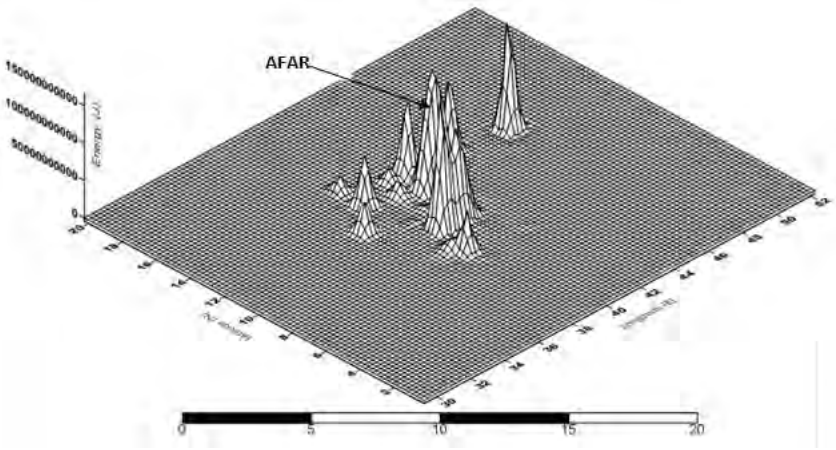

Figure 5.6: Spatial variation of seismic energy release for the period 2000 - 2002. Dominant energy peaks up to 2×10^{11}J are observed in the Ankober - Dofen and Afar.

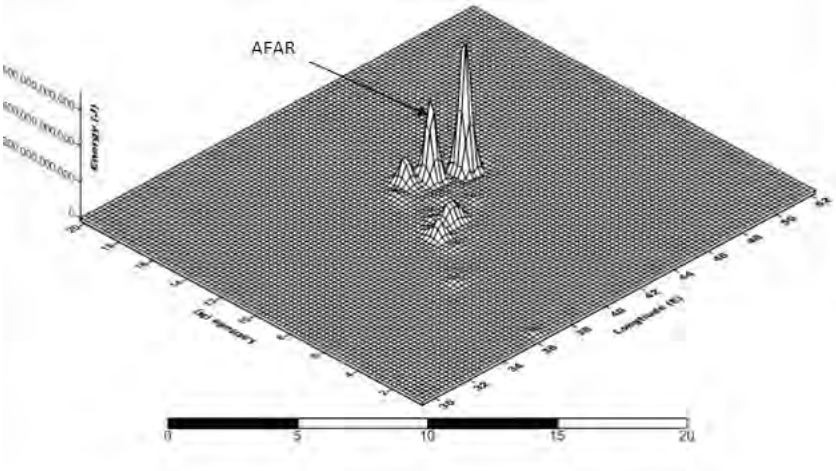

Figure 5.7: Spatial variation of seismic energy release for the period 2000 - 2002 using Brazier et al., 2006. Dominant energy peaks up to 9.9×10^{11}J, are observed in the Ankober - Dofen and Afar.

CHAPTER 6

Discussions

This work presented the results of energy mapping that was conducted in the Afar and The main Ethiopian rift during the time period between 2000 and 2002.

The earthquake catalogue for the time period between 2000 and 2002 given in appendix A is complete above the threshold magnitude 2.75. b - value estimated for the catalogue obtained using the maximum - likelihood method (Aki, 1965 [3]). The error is calculated from the standard deviation of b (Shi and Bolt, 1982 [49]). A relatively higher b-value 0.90 ± 0.09 obtained in this estimation from the slope of the frequency magnitude distribution (FMD) curve shown in Fig 5.2. This implies that the frequency of occurrence of small size earthquake is relatively higher than the bigger ones. Most of the earthquakes in this study have magnitudes between 1 and 2, and the largest is 4.0.

The Gutenberg - Richter cumulative seismicity rate shows the relation $LogN = 4.47 - 0.9 \times M_c$. The FMD curve shows the catalog is only complete to magnitude 2.75. The b - value found in this estimation of 0.9 falls with in the range of values previously reported for MER, Southern Red Sea, Gulf of Aden (Ayele and kulhánek, O. 1997 [9] ; Hofster and Beyth, 2003 [31]; Keir, Stuart, et al., 2006 [36]).

Seismicity is observed near the Ankober border fault where stress is believed to concentrate in this area due to the lateral density and lithosperic thickness contrast between the adjacent plateau and rift (e.g. Tiberi et al.,2005). The epicentral distribution in this area observed can be considered to show the fact that the Ankober Border fault is still experiencing strain (Wolfenden et al.,2004 [53]) exceptionally from the other border faults as also revealed by Keir et al., 2006a [36]. The scattered epicenter distribution for the

study period is also an indication of continued rifting process.

The relatively higher b - value shows that seismic energy in the region is released mainly in the form of low magnitude earthquake. This value shows a relatively higher stress condition in the Ankober - Dofen area. The source of these stresses may be due to the fact that the east African Rift system is in an early stage of rifting as was suggested by Ayele and kulhánek, O. 1997 [9].

Although there is a small difference in earthquake locations mapping between this study and Brazer et al., 2006 (APPENDIX G), it is clearly shows that Brazer et al., 2006 earthquake distribution that is occurred during the time period between 2000 and 2002 is more scattered than as the expected locations in the rift.

Even if the distribution of the epicenters that is located in this research more similar to Brazer's et al, 9 bogus events (Fig 6.2) are found that are reported to occur in the Ethiopian region but never existed in reality (Table 6.1). 6 earthquakes reported events are also found to be telesesmic (Fig 6.1) while they are reported to occur in Afar and the main Ethiopian rift (Table 6.2). 25 poorly located events (less than 3 stations) have found out, see (APPENDIX E). Finlay 53 new events have been identified which is not existed in the catalog, see (APPENDIX D).

From Fig 6.3, it can be seen that the locations of the earthquake events that has been made by this study reveal that most of the epicenters are the expected locations on the rift where as the location made by Brazier et al is more scattered. [1]

[1] In Table 6.2, * represents United States Geological Surevey.

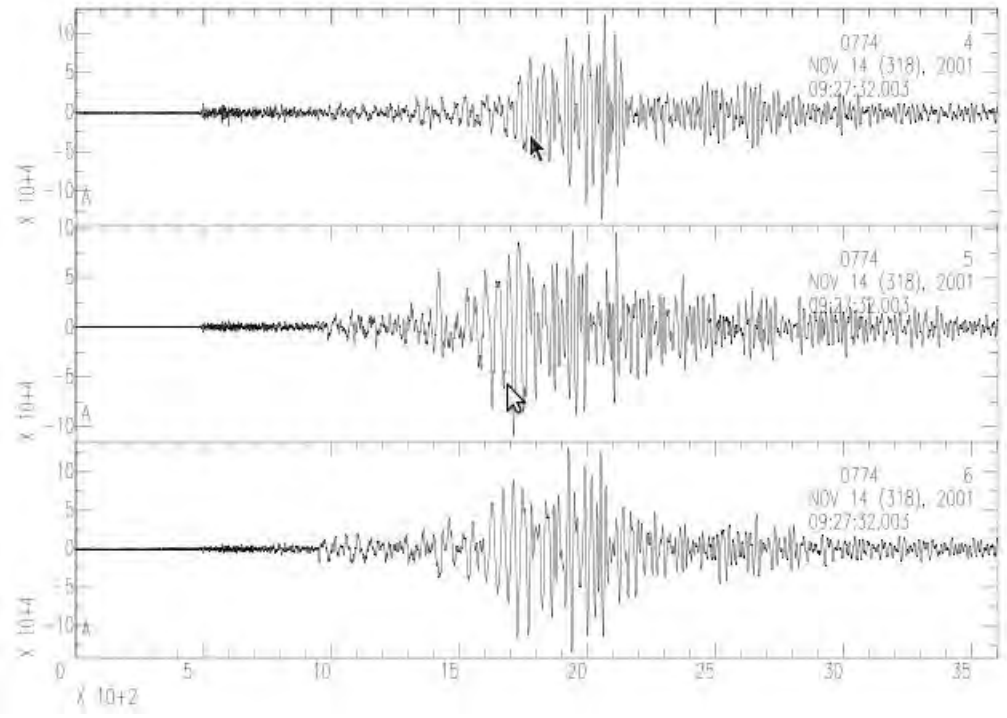

Figure 6.1: This is an example of SAC format unfiltered teleseismic wave form from station Bahir Dar. It is from a Broadband instrument with the vertical component at the top followed by the North - South then East - West component respectively. It is the 2001:11-14; 09:26:10 event with location at latitude of 35.95^0 and longitude of 9.54^0 and a magnitude 7.8 M_w and considered to be a local earthquake by Braizer et al., 2006.

Date	*Time*	*Latitude*	*Longitude*	*Magnitude*
07-26-01	01:10:10	9.341	39.470	2.4
11-09-01	01:06:25	8.214	36.901	2.0
11-12-01	00:47:27	9.395	39.370	1.4
11-21-01	08:33:53	0.730	36.202	3.4
11-21-01	18:57:40	12.188	41.533	2.7
11-30-01	10:28:37	7.891	36.920	2.8
12-10-01	22:47:25	11.768	41.502	2.0
12-25-01	23:19:39	7.196	37.865	1.7

Table 6.1: Bogus events located in the Brazier et al., 2006 catalog

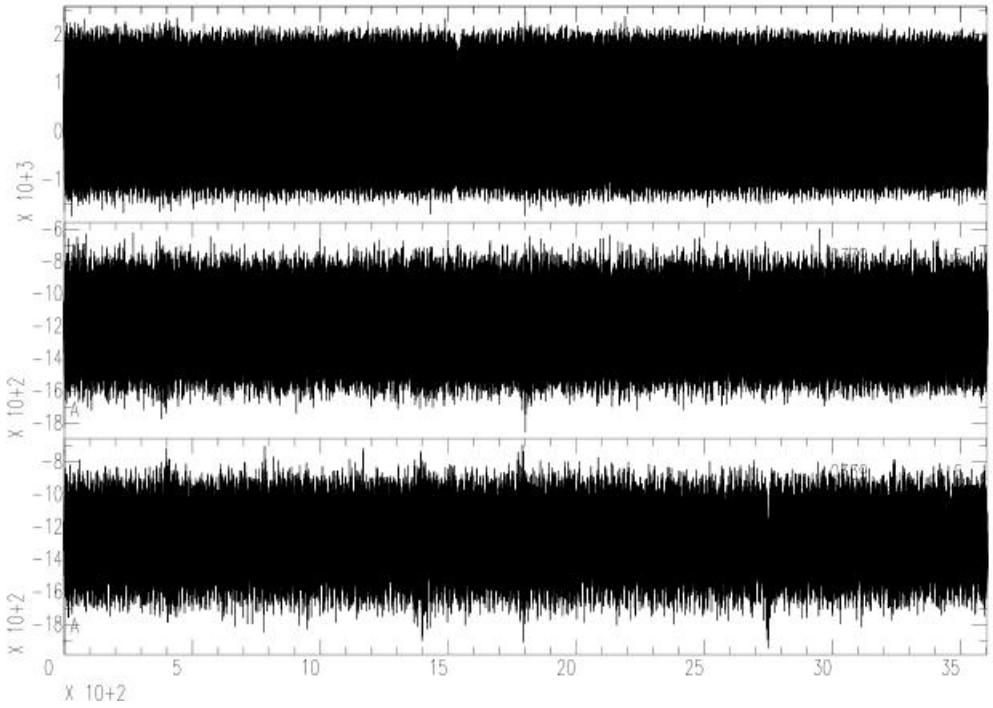

Figure 6.2: This is an example of SAC format unfiltered bogus wave form from station Wash. It is from a Broadband instrument with the vertical component at the top followed by the North - South then East - West component respectively it is the 2001-12-25; 23:19:39 event.

Date $(Month, Date, Year)$	*Time* $(Hr:Mn:Se)$ *Brazier's*	*Time* $(Hr:Mn:Se)$ *U.S.G.S**	*U.S.G.S Latitude* $(degree)$	*U.S.G.S Longitude* $(degree)$	*U.S.G.S Magnitude*
06-24-01	01:35:06	01:22:53	-17.58	-71.96	5.5 M_s
09-16-01	02:06:27	02:00:47	37.24	21.87	5.5 M_w
10-12-01	15:18:47	15:02:16	12.69	144.98	7.0 M_w
11-14-01	09:34:41	09:26:10	35.95	90.54	7.8 M_w
11-23-01	00:33:50	23:22:20	-16.25	178.02	6.3 M_w
		23:24:47	-16.24	178.05	6.2 M_s
12-24-01	01:30:13	22:52:54	-9.61	159.53	6.8 M_w

Table 6.2: Teleseismic events located in the Brazier et al., 2006 catalog.

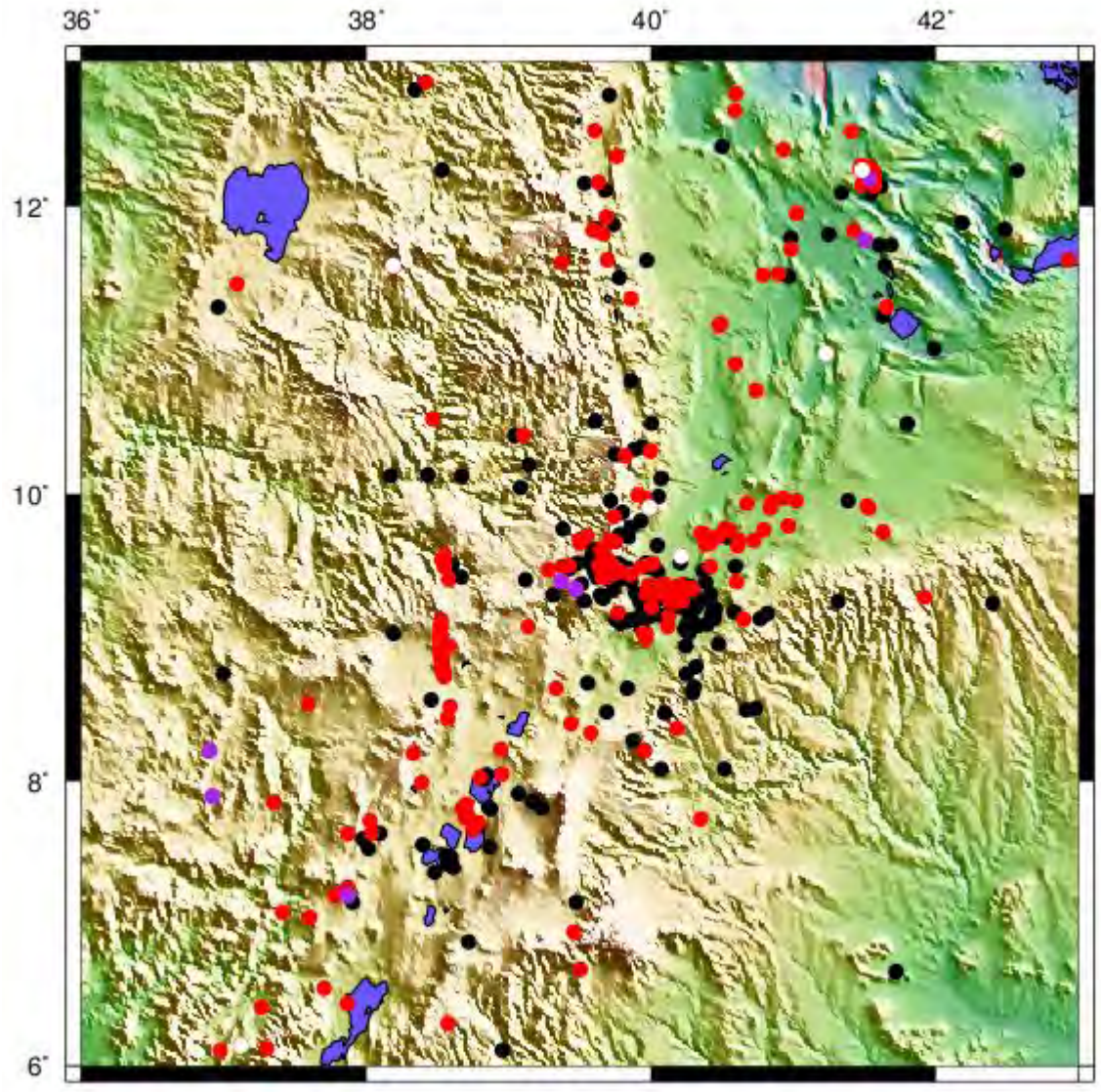

Figure 6.3: The distribution of epicenters located by this study and Brazier et al., 2006 study during the time period between 2000 and 2002. The black colors are location from this study, the red ones are Brazier's locations, the purple ones are the bogus events and the white ones are telesesmic events.

CHAPTER 7

Conclusion and Recomendation

Earthquakes data recorded between 2000 and 2002 are used to study the seismicity of Ethiopia mainly focused around Afar and the Main Ethiopian rift. The major out come of this work is a better catalogue and the seismic energy map produced for the study area. A total of 238 epicentral locations are reported. Locations for earthquakes with in the network were determined with high accuracy. Previous studies of seismicity by Brazier et al., 2006 has been revisited using the same data from IRIS/PASSCAL broadband seismic experiments and adding more from ESSN (Ethiopian Seismic Station Network) sources. When we compare the locations of the earthquake events that has been made by this study and previous studies by Belachew, 2007 and Brazier et al., 2006, this study cover more period of time as compared to Belachew, 2007 which only considered limited period from may to July 2001. Brazier et al locations is more scattered but the present study reveal that most of the epicenters are on the expected locations on the rift.

Comparing the results in this study with Brazier et al., 2006's, it is found that eight bogus events (earthquakes that didn't occur in the real world) and six more teleseismic earthquakes are reported as if they occurred in the Ethiopian neighborhood. On the other hand it is observed that Brazier et al's work, which is published in Bulletins of Seismological Society of America (BSSA), reported 25 earthquakes that are located with readings from seismic stations less than three which puts doubt on the accuracy of the seismicity study. Another 53 new earthquakes are identified in the database and located in this study which has improved details of the seismicity of the region for the time period

considered. Due to the above short comings of Brazier et al's work and Belachew, 2007 the present catalogue is more reveal the seismicity of Afar and the Main Ethiopian rift for the time period 2000 - 2002.

The distribution of epicenter in this study shows high seismic activity around 9^0 N and 40.5^0 E; and 9.5^0 N and 39.5^0 E during the study period, these epicenters are close to the N - S trending Ankober region, Kessem area and Dofen volcano.

The locations of the earthquake events that has been made by this study reveal that most of the epicenters are the expected locations on the rift where as the location made by Brazier et al is more scattered.

The computation results indicate that most of the seismic energy released has been occurred in Ankober - Dofen area. The energy release magnitude suggest that different segments have gone under similar stresses conditions which may in turn reflect the status of the ongoing rifting processes in each segment. Generally these finding could be used for seismic hazard mitigation, land use planning, other development structure and as input for further studies in the fields of geodynamics. Besides in order to understand the clear picture of nature of the rift development different seismological and /or other geophysical approach is recommended like Vertical Electrical Sounding (VES), Magnetics, Seismic refraction using artificial source and so on.

Bibliography

[1] Acocela, V & Korme, T. 2002. Holocene extension direction along the Main Ethiopian Rift, East Africa. Terra Nova, 14, 191 - 197.

[2] ACTA VULCANOLOGICA, Journal of the National Volcanic Group of Italy, Volume 11(1).1999, page 5

[3] Aki, k.,1965. Maximum Likelihood Estimate of b in the Formula log N = a - b×M and its confidence Limits. Bull. Earthq. Res. Inst., 43, pp. 237 - 239.

[4] Aki, K. & Richards, P.G.1980. Quantitative Seismology: Theory and Methods. Volume I.

[5] Ayele, A. 1995. Earthquake catalogue of the Horn of Africa for the period 1960 - 1993; Seismological Dept.,Uppsala Univ., Report, 3-95, 1-9.

[6] Ayele,A.2000. Normal left-oblique fault mechanisms as an indication of sinistral deformation between Nubia and Somalia plates in the Main Ethiopian Rift. J. Afr. Earth Sc., 31 (2), 359-367.

[7] Ayele, A. & Arvidsson, R. 1998. Fault mechanisms and tectonic implication of the 1985- 1987 earthquake sequence in south-western Ethiopia. J. Seismology,1, 383-394.

[8] Ayele, A. & kulhánek, O., 2000. Reassessment of source parameters for three major earthquakes in the East African rift system from historical seismograms and bulletins. Annali Di Geofisica, 43, 81 - 94.

[9] Ayele, A., & kulhánek, O. 1997. Spatial and temporal variations of the seismicity in the Horn of Africa from 1960 to 1993, Geophys. J. Int., 130, 805-810.

[10] Ayele, A., Nyblade, A.A, Langston, C.A., Cara, M. and Leveque, J. 2006. New evidence for Afro-Arabian plate separation in southern Afar. In: Yirgu, G., Ebinger, C.J., and Maguire, P.K.H. (eds) The Afar volcanic province within the east African Rift system Geol. Soc. London, Special Publications, 259, 133-141.

[11] Ayele, A., Stuart, G., Bastow, I. & Keir, D. 2007. The August 2002 earthquake sequence in north Afar: Insights into the neotectonics of the Danakil microplate. J. Afr. Earth Sc., 48, 70 - 79.

[12] Bastow, I., Stuart, G., Kendall, M. & Ebinger, C.J. 2005. Upper mantle seismic structure in a region of incipient continental break-up: northern Main Ethiopian Rift. Geoph. J. Int., 162, 479 493.

[13] Båth, M.,1979 . Introduction to Seismology, Second, Revised Edition,page 120

[14] Baxter C.D. Chimlambe. 2008. Seismicity of East Afican Rift system from 2000 - 2007,un published thesis, Addis Ababa University.

[15] Belachew. 2007. Seismotectonics of the Ethiopian Rift From some selected earthquakes in 2001 ,un published thesis , Addis Ababa university.

[16] Bilham, R., Bendick, R., Larson, K., Mohr, P., Braun, J., Tesfaye, S. & Asfaw, L.M. 1999. Secular and tidal strain across the Ethiopian Rift. Geoph. Res. Lett., 26, 2789 2792.

[17] Boccaletti, M., Bonini, M., mazzuoli, R., Abebe, B., Piccardi, L. & Tortorici, L.1998. Quaternary oblique extensional tectonics in the Ethiopian Rift (Horn of Africa). Tectonophysica, 287, 97 116.

[18] Casey, M., Ebinger, C.J., Keir, D., Gloaguen, R. & mohamed, F. 2006. Strain accommodation in transitional rifts: extension by magma intrusion and faulting in Ethiopian rift magmatic segments. In: Yirgu, G., Ebinger, C.J., and Maguire, P.K.H. (eds) The Afar volcanic province within the east African Rift system. Geol. Soc. London, Special Publications, 259, 143 - 163.

[19] Chu, D. & Gordon, R. 1999. Evidence for motion between Nubia and Somalia along the Southwest Indian ridge. Nature, 398, 64 - 66.

[20] Dugda, M., Nyblade, A.A., Julia, J., Langston, C.A., Ammon, C.J. & Simiyu, S. 2005. Crustal structure in Ethiopia and Kenya from receiver function analysis: Implications for rift development in eastern Africa. J. Geoph. Res., 110,

[21] Ebinger, C.J. & Casey, M. 2001. Continental breakup in magmatic provinces: an Ethiopian example. Geol., 29, 527 - 530.

[22] Ebinger, C.J., Yemane, T., Harding, D., Tesfaye, S., Rex, D. & Kelly, S. 2000. Rift deflection, migration, and propagation: Linkage of the Ethiopian and eastern rifts, Africa. Geol. Soc. Am. Bull., 102, 163 - 176.

[23] fairhead & girdler, 1971. The seismicity of east African rift system.

[24] Fowler C.M.R. The Solid Earth,An Introduction Global Geophysics. 1995.

[25] Frohlich, C., and SD Davis (1993). International handbook of earthquake and engineering seismology.

[26] Ghebreab, W.1998. Tectonics of the Red Sea region reassessed, Earth-Science Reviews 45-1998. 1-44

[27] Gouin, P. 1979. Earthquake history of Ethiopia and the Horn of Africa. International Development Research Center, Ottawa, Ont., pp. 258.

[28] Gutenberg, B. & Richter, C.F. 1956. Earthquake magnitude, intensity, energy, and acceleration. Bull. Seism. Soc. Am., 46, 105-145.

[29] Havskov, J. & Ottemoller, L. 2000. SEISAN: The Earthquake Analysis Software. Inst. Solid Earth Physics, Univ. Bergen.

[30] Hofmann, C., Courtillot, V., Feraud, G., Rochette, P., Yirgu, G., Ketefo, E. and Pik, R. (1997) Timing of the Ethiopian flood basalt event and implications for plume birth and global change. Nature, 389, 838 - 841.

[31] Hofstetter, R. & Beyth, M. 2003. The Afar Depression: interpretation of the 1960 2000 earthquakes. Geoph. J. Int., 155, 715 732.

[32] Kasahara ,1981. Earthquake Mechanics.

[33] Kebede, F. 1989. Seismotectonics of the East African rift system north of 12 S to southern Red Sea. Seismological Dept., Uppsala Univ., Report No. 1-89, pp. 34.

[34] Kebede, F., Kim, W.-Y. & kulhánek, O. 1989. Dynamic source parameters of the March- May 1969 Serdo earthquake sequence in Central Afar, Ethiopia, deduced from teleseismic body waves. J. Geoph. Res., 94, 5603 - 5614.

[35] Kebede, F. & kulhánek, O. 1994. Spatial and temporal variations in b-values along the East African rift system and the southern Red Sea. Phys. Earth Planet Inter., 83, 249- 264.

[36] Keir, D., Ebinger, C.J., Stuart, G., Daly, E. & Ayele, A. 2006a. Strain accommodation by magmatism and faulting as rifting proceeds to breakup: Seismicity of the northern Ethiopian Rift. J. Geoph.Res., 111, B05314, doi:1029/2005JB 003748.

[37] Keir, D., Stuart, G.W., Jackson, A. & Ayele, A 2006b. Local earthquake magnitude scale and seismicity rate for the Ethiopian rift. Bull. Seism. Soc. Am., 96, 1-10.

[38] Keranen, K., Klemperer, S., Gloaguen, R. & EAGLE working group. 2004. Three-dimensional imaging of a protoridge axis in the Main Ethiopian Rift. Geol., 39, 949 - 952.

[39] Lay, T. & Wallace, T.C. 1995. Modern global seismology. Academic Press San Diego, California.

[40] Mackenzie, G., Thybo, H. & Maguire, P.K.H. 2005. Crustal velocity structure across the Main Ethiopian Rift: Results from two-dimensional wide-angle seismic modelling. Geoph. J. Int, 162, 994 - 1006.

[41] McKenzie, D.P., Davies, D. & Molnar, P., 1970. Plate tectonics of the Red Sea and East Africa. Nature, 226, 243-248.

[42] Menzies, M., Baker, J., Bosence, D., Dart, C., Davison, I., Hurford, A., AlKadasi, M., McClay, K., Nichols, G., AlSubbary, A., and Yelland, A., 1992; The timing of magmatism, uplift and crustal extension: Preliminary observation from Yemen, in Storey, B.C., Alabaster, T., and Pankhurst, R.J., eds, Magmatism and the causes of continental break-up. Geological Society of America Special Paper, 68, 293304.

[43] Mohr, P.A. 1967. The Ethiopian Rift system. Bull. Geoph. Obser. Addis Ababa 11, 1 - 65.

[44] Mohr, P.A. 1987. Patterns of faulting in the Ethiopian Rift Valley. Tectonophysics, 143 169 - 179.

[45] Nolet, G., & Muller, S 1982, A model for the deep structure of the East African Rift system from simultaneous inversion of teleseismic data, Tectonophysics, 84, 151 - 178.

[46] Nyblade, A.A. & Langston, C.A. 2002. Broadband Seismic experiments probe in East African rift. Eos Trans. AGU, 83, 405-410.

[47] R. A. Brazier, Q. Miao, A. A. Nyblade, A. Ayele, & C. A. Langston.2006. Local Magnitude Scale for the Ethiopian Plateau Bulletin of the Seismological Society of America, Vol. 98, No. 5, pp. 23412348, October 2008, doi: 10.1785/0120070266.

[48] Schilling, J.-G, Kingsley, R., Hanan, B. and McCully, B. 1992. Nd-Sr-Pb isotopic variations along the Gulf of Aden: Evidence for the Afar mantle plume-lithosphere interaction. J. Geophys. Res., 97, 10927 10966.

[49] Shi & Bolt (1982). T H E STANDARD ERROR OF THE MAGNITUDE - FREQUENCY b VALUE. Bulletin of the Seismological Society of America, Vol. 72, No. 5, pp. 1677-1687, October 1982

[50] Teshome, 2007- Source Characterization of the may 2000 southern Afar earthquake sequence,un published thesis(2007),Addis Ababa University.

[51] [Wiemer & McNutt, 1997. Spatial Variations in the Frequency-Magnitude Distribution of Earthquakes.

[52] WoldeGabriel, G., Aronson, J. & Walter, R. 1990. Geology, geochronology, and rift basin development in the central sector of the Main Ethiopian Rift. Geol. Soc. Am. Bull., 102, 439 - 458.

[53] Wolfenden, E., Ebinger, C.J., Yirgu, G., Deino, A. & Ayalew, D. 2004. Evolution of the northern Main Ethiopian Rift: birth of a triple junction. Earth and Planetary Science Letters, 224, 213 228.

[54] Yirgu, G .2006, The Afar volcanic province within the East African Rift System: Inroduction, Geological Society, London, Special Publicaiton; V.259;1-6

Appendix

7.1 Appendix A ...Catalogue of earthquakes located in this study

Catalogue of earthquakes located in this study

DATE - Date of the event (year/month/day)
OR. TIME - Event origin time in GMT (Hour:Minute:Second)
LAT. - Latitude of the earthquake epicenter in degrees
LON. - Longitude of the earthquake epicenter in degrees
MC.- Coda magnitude
DEP.- Depth in km
NST.- Number of stations used
RMS.- Root mean square error

Table 7.1 below shows the catalog of earthquakes located in this study.

DATE	*OR.TIME*	*LAT.*	*LON.*	*DEP*	*NST*	*RMS*	*MC*
00/06/21	16:51:54	7.415	38.573	0.1	4	0.7	3
00/06/21	21:48:55	7.479	38.555	0	4	1.3	3.7
00/06/21	22:16:38	7.467	38.591	0	4	1.2	2.8
00/06/27	01:26:46	9.956	41.386	0	3	1	3
00/08/30	11:19:37	9.423	38.668	0	3	0.8	3.2
00/09/12	17:41:42	11.302	36.958	28.6	4	0.4	2.1
00/09/28	17:58:41	10.492	41.801	0	5	1.3	3.1
00/11/17	04:34:11	7.553	38.396	0.1	3	0.7	2.7
01/05/04	00:26:34	12.159	39.534	0.1	3	1.2	2.8

DATE	*OR.TIME*	*LAT.*	*LON.*	*DEP*	*NST*	*RMS*	*MC*
01/05/10	16:50:05	6.662	41.721	2	4	1.2	2.9
01/05/12	01:44:14	9.49	39.699	0	9	1.1	2.8
01/05/12	02:06:43	9.573	39.669	0	10	0.8	2.6
01/05/12	02:46:54	9.442	39.802	0	5	1	2.1
01/05/12	04:00:54	9.123	39.833	0	6	0.4	1.2
01/05/14	05:16:06	9.278	39.667	0	3	0.4	2.1
01/05/18	20:32:57	7.631	38.097	0	9	1.2	2.4
01/05/19	17:54:33	7.15	39.473	50	3	0.8	2.6
01/05/19	18:48:26	12.875	46.76	2	4	1.9	4
01/05/21	20:09:10	9.702	39.839	0.4	7	0.8	1.7
01/05/22	16:10:20	9.267	40.138	0.5	6	1.4	2.3
01/05/22	01:16:10	9.484	39.429	0.1	15	0.6	3.2
01/05/24	08:09:52	9.516	39.72	0	8	0.9	2.5
01/05/24	20:24:37	9.502	39.416	2.7	7	0.7	1.7
01/05/24	21:25:52	9.359	40.28	3	5	0.5	2
01/05/26	20:10:45	11.732	41.686	8.7	7	0.9	2.9
01/05/28	07:39:03	6.106	38.955	0	3	0.3	2.9
01/05/30	20:19:14	9.192	39.983	3	5	0.8	2.1
01/06/02	23:09:51	7.147	37.904	113.7	4	1	2.5
01/06/04	11:38:27	9.262	40.266	0	6	0.8	2.4
01/06/04	22:56:19	9.288	40.303	0	11	1.2	2.6
01/06/04	23:12:22	9.286	40.297	1.9	9	0.9	2.9
01/06/05	01:58:40	9.095	40.398	9.1	6	1.1	2.3
01/06/08	01:24:58	10.13	38.171	50	4	1.5	2.7
01/06/08	05:00:03	11.876	39.735	6.2	4	0.1	1.8
01/06/14	05:16:16	9.476	39.604	0	5	0.7	2.5
01/06/14	23:32:28	7.804	38.875	0	6	0.5	2.4
01/06/15	01:09:23	7.813	38.86	0	4	1	2.4
01/06/17	23:54:55	9.308	40.258	15.2	7	0.8	2
01/06/19	22:56:29	9.186	40.269	0	5	0.6	2.8
01/06/22	11:27:05	9.138	40.444	0.1	4	0.6	1.7
01/06/22	14:09:20	8.613	40.293	0	4	0.9	2.8
01/06/22	14:52:29	9.253	40.247	0	8	0.8	2.9

DATE	*OR.TIME*	*LAT.*	*LON.*	*DEP*	*NST*	*RMS*	*MC*
01/06/22	23:39:58	9.245	40.305	0.1	12	0.5	3.2
01/06/23	13:20:45	9.04	39.956	0.1	6	0.3	3.2
01/06/23	19:09:08	9.237	40.309	0	13	0.9	3.1
01/06/23	19:12:07	9.275	40.394	0.9	5	1	3.4
01/06/23	20:00:25	9.497	40.594	0.1	9	1.3	3.7
01/06/24	01:47:22	9.172	40.267	20.4	9	0.8	2.8
01/06/24	02:19:40	9.158	40.425	19.3	5	0.5	3
01/06/24	03:53:25	9.268	40.198	6.6	6	1.1	2.5
01/06/24	07:26:37	9.206	40.45	0	5	1	2.5
01/0/624	10:46:03	9.469	40.367	27.4	6	1.5	2.7
01/06/24	13:21:37	9.262	40.409	0	8	0.5	2.8
01/06/24	18:17:28	9.177	40.443	0	6	0.6	2.1
01/06/24	18:22:57	9.302	40.419	3	7	0.4	3
01/06/24	20:25:41	9.296	40.301	7	5	1.5	2.8
01/0/625	04:07:31	9.225	40.302	0	7	0.6	2.8
01/06/25	07:37:54	9.272	40.226	7.2	5	1.3	3.2
01/06/25	08:26:19	9.285	40.158	0	7	0.6	2.9
01/06/25	09:14:48	9.25	40.317	0	9	0.7	3.4
01/06/25	09:46:09	9.214	40.314	3	7	0.6	3
01/06/25	10:20:47	9.06	40.238	53.4	5	1.2	2.1
01/06/25	16:37:54	8.497	40.667	31	6	0.6	2.7
01/06/25	16:39:51	9.096	40.281	30	5	0.7	2.1
01/06/25	16:52:57	9.387	40.387	3	4	0.7	2.5
01/06/25	16:59:55	9.254	40.243	20.4	7	0.9	2.4
01/06/25	17:03:05	9.145	39.981	3	7	1	3.3
01/06/25	17:36:13	9.212	40.302	16.7	5	0.7	2.9
01/06/26	12:46:53	9.299	40.204	0	8	1.1	2.7
01/06/26	17:33:26	9.06	39.935	1	5	1.2	3.1
01/06/26	17:39:53	9.271	40.279	17.9	6	1	3.1
01/06/26	22:22:07	9.253	40.192	6.4	12	1.3	3.2
01/06/26	23:42:23	9.268	40.202	1	6	1.3	2.4
01/06/27	01:05:03	8.957	40.474	2	8	1.8	3
01/06/27	10:40:14	8.748	40.247	40.9	3	0.5	2.8
01/06/27	15:14:21	9.095	40.254	2	4	1	2.9
01/06/28	07:13:43	8.483	39.69	0	4	0.2	2.7
01/06/28	23:48:13	8.282	39.873	83.6	5	1.1	2.7
01/06/29	14:44:25	8.659	40.305	24.4	4	0.1	3.1
01/06/30	08:48:01	9.243	40.274	0	7	0.7	3.1
01/07/01	15:15:55	9.182	40.58	21.4	3	0.7	3
01/07/01	17:24:52	9.086	40.334	12.6	4	0.7	2.9
01/07/02	01:37:34	9.16	40.435	30.2	6	0.3	2.7
01/07/02	19:48:36	9.34	40.19	3.2	5	1	2.6

DATE	*OR.TIME*	*LAT.*	*LON.*	*DEP*	*NST*	*RMS*	*MC*
01/07/02	21:00:58	9.335	40.202	15.8	6	0.6	2.2
01/07/05	09:49:07	9.205	40.233	0	8	0.7	2.8
01/07/09	21:03:20	9.165	40.283	1.4	7	0.9	3
01/07/09	23:24:07	9.126	39.753	0	9	1.3	2.7
01/07/13	22:34:11	9.132	40.768	0	10	1.2	3.1
01/07/17	18:25:54	7.594	37.978	0.1	6	1	3
01/07/17	18:27:21	13.129	39.024	163.8	5	0.6	2.0
01/07/26	20:20:56	9.957	39.716	8.3	3	1.1	2.3
01/08/03	19:04:13	9.523	39.963	0	8	0.9	2.8
01/08/04	11:51:09	9.22	40.306	0	3	0.5	1.1
01/08/04	12:59:05	10.206	39.139	40.2	6	1.3	2.5
01/08/07	00:07:21	9.396	39.859	9.8	5	0.3	2.7
01/08/07	10:56:35	8.799	40.316	2	4	0.7	2.4
01/08/14	05:02:57	9.247	40.27	0.1	5	0.5	2.9
01/08/17	21:30:25	10.791	39.861	56.4	4	1.2	2.5
01/08/21	21:42:27	9.368	40.237	0	6	0.9	2.8
01/08/25	22:34:23	9.441	39.648	0	7	0.8	2.1
01/08/30	18:03:48	9.988	40.052	0	6	0.5	2.7
01/09/01	18:07:26	10.111	40.069	0.3	11	0.9	2.9
01/09/02	13:08:55	9.443	39.799	0	7	0.9	2.1
01/09/08	07:57:18	9.497	39.975	3	3	0.2	2.1
01/09/08	11:24:11	9.677	40.42	0	3	0.7	2.5
01/09/11	19:04:45	9.396	39.752	8	7	0.9	2.2
01/09/13	9:37:02	10.331	39.935	0	4	0.4	2.1
01/09/13	17:51:28	10.279	39.748	0	5	0.3	3.2
01/09/18	01:46:25	9.102	39.784	0.1	8	0.6	2.9
01/09/18	23:34:43	9.24	42.401	7.8	8	0.4	2.7
01/10/03	10:56:02	12.111	39.678	0	4	0.1	3.2
01/10/03	17:42:54	8.749	36.997	8	6	1	2.7
01/10/06	18:29:45	9.519	39.48	0	4	0.3	2.5
01/10/08	05:51:47	9.703	40.536	0.1	4	1.5	3.3
01/10/09	03:06:16	11.628	39.969	0	9	0.8	3.1
01/10/09	10:12:13	12.767	39.708	52.5	4	0.3	2.7
01/10/14	20:12:20	11.846	39.613	0	4	1.3	2.1
01/10/14	18:53:32	9.511	38.599	8.1	5	0.5	2.3
01/10/20	20:50:51	9.312	39.893	0.1	3	0.5	1.7
01/10/22	04:35:46	10.496	40.003	0	3	0.6	2.0
01/10/22	15:11:32	9.72	39.786	1.7	5	0.7	3.2
01/10/24	02:26:55	9.125	39.873	0	6	1.3	3.1
01/11/02	03:50:59	11.782	40.983	1.6	6	1.3	3
01/11/02	06:35:32	8.473	40.098	117	6	0.7	3
01/11/02	16:24:13	11.512	40.965	0	9	0.7	3.7

DATE	*OR.TIME*	*LAT.*	*LON.*	*DEP*	*NST*	*RMS*	*MC*
01/11/02	23:04:25	9.441	39.704	0.1	7	0.5	2.3
01/11/06	21:52:02	8.568	38.454	0.4	4	0.4	2.4
01/11/10	04:38:28	9.674	39.537	0	3	0.5	1.9
01/11/11	02:19:23	9.428	39.684	0	7	0.8	1.6
01/11/11	21:05:23	9.48	39.717	0	9	0.6	1.8
01/11/11	22:32:43	9.468	39.721	2.9	15	0.9	2.8
01/11/11	22:38:01	9.42	39.622	0.7	13	0.6	3
01/11/11	23:00:49	9.446	39.728	0	5	0.6	2.3
01/11/11	23:14:25	9.417	39.795	0	6	0.6	1.7
01/11/11	23:35:45	9.491	39.681	0	9	0.6	2.1
01/11/11	01:56:52	9.457	39.715	1.3	12	0.7	1.9
01/11/12	18:25:55	9.454	39.607	12.9	4	0.3	1.7
01/11/14	06:09:01	10.137	38.435	2.7	6	0.6	2.6
01/11/14	22:53:18	9.436	39.705	0.5	5	0.5	1.6
01/11/17	03:28:18	9.296	40.062	0	9	0.9	2.3
01/11/17	11:34:01	9.489	40.012	49.9	6	0.1	2.6
01/11/18	19:12:08	9.524	40.205	0.1	9	0.9	2.1
01/11/19	02:13:33	8.686	39.554	6.6	7	1.3	2.5
01/11/19	03:08:12	9.13	39.778	6.8	3	0.9	2.2
01/11/19	03:58:20	9.327	40.07	0	9	0.8	2.3
01/11/19	15:44:54	9.30	40.00	1.2	8	0.9	2.2
01/11/19	21:32:04	8.082	40.515	0	5	0.3	2.1
01/11/20	18:39:23	8.648	39.832	7.3	6	1	2.2
01/11/21	18:30:16	11.238	41.629	20.3	8	0.6	3.7
01/11/21	21:30:18	14.257	38.44	0	7	0.5	3.5
01/11/21	23:58:31	11.807	41.248	11	11	0.7	4
01/11/23	09:04:38	9.329	40	1	8	0.7	2.4
01/11/23	14:45:33	9.251	39.924	23.2	12	1	2.9
01/11/24	01:12:58	9.322	40.019	3	6	0.7	2.2
01/11/24	13:03:37	10.128	38.669	12.6	9	1.3	3
01/11/25	05:30:38	11.59	41.643	0	8	0.4	3.9
01/11/25	12:48:27	12.248	42.57	0	6	0.8	3.3
01/11/25	14:47:55	11.887	42.186	39.7	8	0.9	2.3
01/11/25	20:38:43	12.09	41.544	0	3	0.7	2.5
01/11/26	20:59:40	7.359	38.483	2	3	0	1.6
01/11/27	21:35:38	9.452	39.696	2.6	9	0.9	2.3
01/11/28	03:51:57	9.155	40.065	8	4	1	2.3
01/11/29	20:27:12	9.368	40.039	0.1	14	1	2.8
01/11/29	21:14:29	9.271	40.049	8	4	0.9	1.8
01/11/30	00:35:04	9.305	40.114	0	5	0.7	1.8
01/11/30	00:43:01	9.267	40.007	0	5	0.7	2.1
01/11/30	00:44:34	9.22	40.009	0	7	0.8	1.8

DATE	*OR.TIME*	*LAT.*	*LON.*	*DEP*	*NST*	*RMS*	*MC*
01/12/01	03:16:58	7.853	39.171	2	5	1.3	2.1
01/12/02	12:59:48	10.314	39.882	0	4	0.3	2.0
01/12/03	01:35:51	11.011	41.989	2	3	0.8	2.4
01/12/05	15:52:27	13.415	41.319	0	14	1	3.9
01/12/07	00:52:02	9.375	39.51	2.6	5	0.9	2.1
01/12/08	20:41:51	10.408	39.046	0	7	1.2	2.7
01/12/09	20:00:53	9.184	40.133	0	5	0.8	2.1
01/12/10	10:48:03	13.094	43.97	21	7	0.6	3.9
01/12/10	20:19:16	9.409	39.701	0.1	9	0.7	2.1
01/12/11	0:08:47	9.519	39.77	0	4	0.7	2.3
01/12/11	0:27:35	9.461	39.689	0	7	0.9	1.8
01/12/11	07:01:37	9.029	38.193	0	4	0.5	2.8
01/12/11	21:06:35	9.463	39.639	0.1	6	0.8	1.7
01/12/11	23:11:06	9.475	39.737	0	5	1	1.8
01/12/13	01:11:47	7.8	39.233	2.8	5	0.6	1.9
01/12/13	02:14:36	9.301	39.31	31.9	11	0.8	2.9
01/12/13	21:31:15	9.759	39.38	0	3	0.4	1.5
01/12/18	21:32:32	12.25	38.535	15.9	5	1.2	1.9
01/12/20	4:31:25	10.049	39.08	19.1	5	0.4	1.9
01/12/20	11:07:39	9.284	39.656	4	3	0.6	2.1
01/12/21	0:53:56	9.469	39.634	0.1	4	0.5	2.2
01/12/21	01:34:45	9.334	39.733	1.9	3	0.6	2
01/12/22	00:57:19	9.257	39.528	0.7	4	0.5	1.9
01/12/23	22:33:37	7.683	38.786	0	5	1	2
01/12/24	08:33:52	12.413	40.501	13.3	3	0.1	3
01/12/24	08:56:18	12.092	41.336	0	3	0.5	3.8
01/12/25	03:52:49	9.301	39.646	3	6	0.7	2.1
01/12/26	0:20:39	7.536	38.867	7.5	8	0.7	2.4
01/12/27	05:30:56	8.044	38.845	7.9	5	1	2.2
01/12/27	05:35:35	8.01	38.826	13.5	5	0.6	2.9
01/12/27	08:48:40	7.9	39.069	56.7	4	1.4	2.9
01/12/28	21:37:38	9.461	40.048	86.7	5	0.7	2.2
01/12/30	06:16:16	9.437	39.663	0	5	0.9	2.3
01/12/30	18:59:58	9.442	39.661	3	5	0.6	2.4
01/12/31	02:17:09	9.818	39.928	8.8	3	1	2.5
02/01/02	21:03:26	8.507	40.732	0	4	1	2.6
02/01/03	03:52:28	9.645	40.043	0.1	4	0.9	1.6
02/01/03	10:34:10	9.03	40.267	112.3	4	1.2	2.1
02/01/03	14:57:01	9.171	40.82	89.9	4	0.8	2.7
02/01/07	19:21:47	11.505	39.778	0	3	0.2	2.5
02/01/08	22:18:38	9.588	39.589	2.9	3	0.6	2.3
02/01/09	22:18:44	9.718	39.778	3	6	1.3	1.7

DATE	*OR.TIME*	*LAT.*	*LON.*	*DEP*	*NST*	*RMS*	*MC*
02/01/14	22:45:59	9.613	39.608	0.1	5	0.7	1.8
02/01/14	23:34:23	9.487	39.836	0.1	4	0.8	1.3
02/01/15	00:55:49	9.502	39.698	0	6	0.7	2
02/01/17	17:48:22	9.503	39.703	3	7	0.5	2.1
02/01/17	20:01:06	7.524	38.016	0	4	0.4	1.6
02/01/17	20:07:36	9.501	39.792	0	4	1	2.2
02/01/17	20:24:22	9.453	39.669	0.1	7	1	1.9
02/01/17	22:44:00	9.467	39.683	2.3	8	0.9	2.1
02/01/18	01:42:39	8.941	40.243	42.1	7	0.8	2.3
02/01/18	15:43:26	8.083	40.071	110.9	4	1.1	2.5
02/02/07	18:44:41	10.512	39.612	0	9	1	3.1
02/02/11	13:56:38	9.407	39.118	0.1	3	0.4	4
02/02/13	00:38:22	9.256	41.315	2	3	0	2.9
02/02/13	08:48:05	12.805	38.342	0	4	0.4	3.8
02/02/13	23:25:53	11.841	42.485	0	5	0.8	2.7
02/02/17	02:38:12	9.502	39.949	0	4	1	2.4
02/02/17	02:42:15	9.168	39.933	0	4	1	1.9
02/02/21	08:21:59	7.392	38.611	0	7	0.8	1.9
02/02/25	20:45:33	9.772	39.859	2.8	3	0.9	1.7
02/03/01	18:00:08	9.448	39.672	1.2	7	0.8	2
02/03/01	19:14:56	9.438	39.658	0	4	0.7	1.9
02/03/01	20:56:25	9.878	39.801	0	8	1.1	2.9
02/03/01	23:37:50	9.529	39.558	0.1	5	0.7	2.2
02/04/24	23:23:59	6.87	38.719	2.8	3	0.5	2.3
02/05/14	18:49:31	12.141	41.615	0.1	4	0.3	2.0
02/05/16	21:09:56	13.461	40.843	0	3	0.2	2.0
02/05/18	2:00:09	13.409	40.342	29.2	5	0.1	3.5

Table 7.1: Catalogue of earthquakes located in this study

7.2 Appendix B ...Flow chart for an algorithm of energy mapping

The flow chart shown below an algorithm of energy mapping for the study area

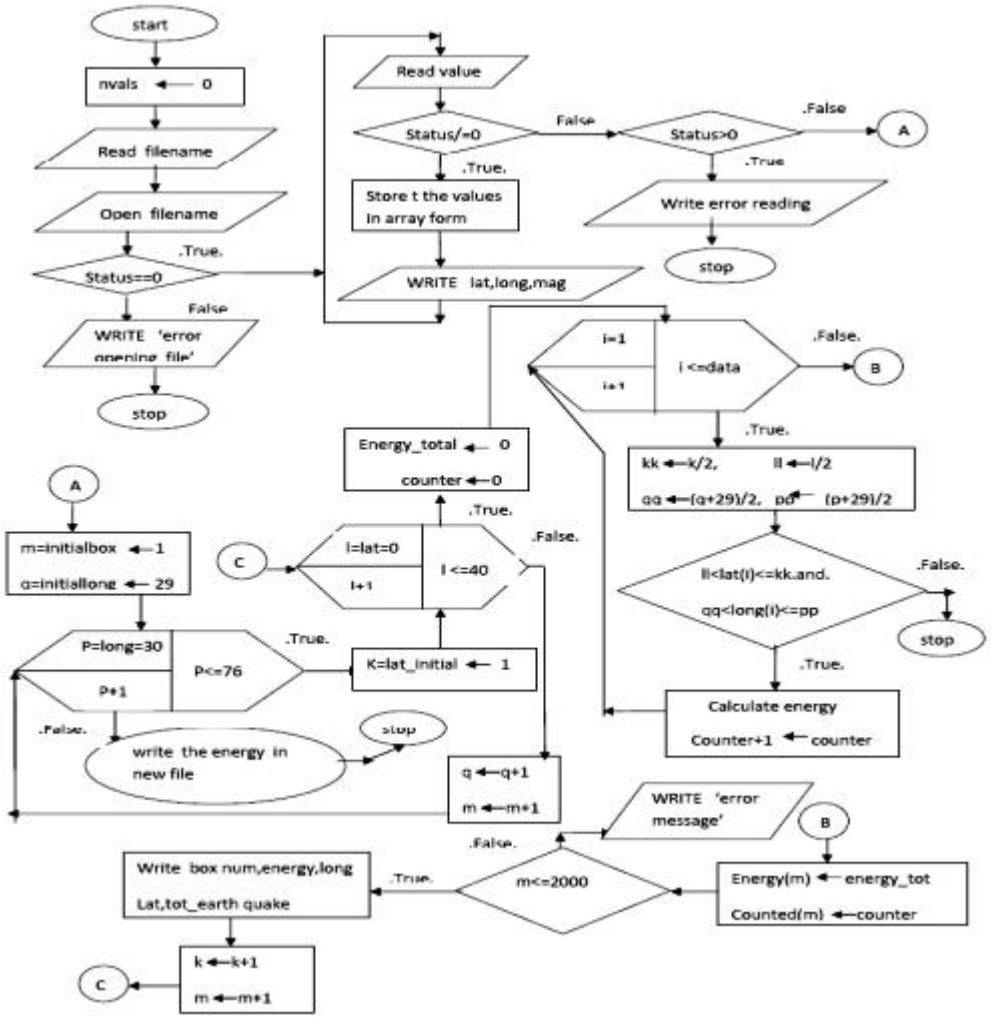

Figure 7.1: Algorithm of energy mapping for the study area.

7.3 Appendix C ...FORTRAN program code for seismic energy mapping

The FORTRAN program code for seismic energy mapping of the study area.

!FORTRAN code for spatial distribution of seismic energy mapping for horn of Africa($0^0 - 20^0$)N and ($29^0 - 52^0$)E

```
PROGRAM ENERGYMAPPING
IMPLICIT NONE
!.....
! Declaration of variables and constants
!.....
INTEGER,PARAMETER::datasize= 2000
INTEGER,PARAMETER::Maxblocks= 2500
CHARACTER(len= 20)::filename
LOGICAL::exceed=.FALSE.
INTEGER::status,counter,nvals= 1
INTEGER::m,p,q,l,k,i
REAL::latitude,longitude,magnitude,j,t
REAL::kk,ll,pp,qq ,w,z
REAL::energytotal,energyindv
REAL,DIMENSION(Maxblocks)::energy
INTEGER,DIMENSION(Maxblocks)::counted
REAL,DIMENSION(datasize)::lat,long,mag
REAL,DIMENSION(0:40,30:76)::site
!.....
! Reading of data from file and store the results in array form
!.....
WRITE(*,*)"please enter the input file name that contains the earth quake data ?"
READ(*,*)filename
OPEN(UNIT=3,FILE=filename,STATUS='old',ACTION='read',IOSTAT=status)
outer: IF(STATUS==0)THEN
reading:DO
READ(3,*,IOSTAT=STATUS)latitude,longitude,magnitude
IF(STATUS/=0)EXIT
nvals=nvals+1
size:IF( nvals<=datasize) THEN
```

```
lat(nvals)=latitude
long(nvals)=longitude
mag(nvals)=magnitude
ELSE
exceed=.TRUE.
END IF size
End DO reading
toobig:IF( exceed)THEN

    WRITE(*,272)nvals-1,datasize
272 FORMAT('maximum array size exceeded:',I6,'>',I6)

    Else
WRITE(*,1030)nvals-1
1030 FORMAT (' ','there are ',I6,3X,"nubere of earthquake in the data.")
2001 FORMAT (X,T15,'SEISMIC ENERGY MAPPING RESULT')
WRITE(*,67)
67 FORMAT (X,T15,'...../)
write(*,*)"To see the out put ,refer the filecalled result.txt "
End IF toobig
inner: IF(status>0)THEN

    WRITE(*,1020)nvals+1
1020 FORMAT (' ','an error occurred reading line',I6)
End IF inner
END IF outer
CLOSE(UNIT=3)
!.....
Calculation of Seismic energy
!.....
open(unit=10,file='result.txt',action='write',status='replace' ) !to output the computed
result in 'result.txt' file

    m= 1;q=29 ! the first grid and intial longtiude respectively
row: DO p=30,76 ! the row correspond to longtiude
k=1
column: DO l=0,40 ! latitude range
energytotal=0 ;counter=0
cheker:DO i=1,datasize qq=q-(q-29)/2.0 ; ll=l-l/2.0 ; kk=k-k/2.0 ; pp=(p+29)/2.0 ! 0.5
```

```
by 0.5 grid

    IF(ll<=lat(i).AND.lat(i)<=kk.AND.qq <=long(i).AND.long(i)<=pp)Then

    energyindv=10**(2.9825 + 2.124 *mag(i)) !using regression relation of mb and mc
energytotal= energytotal+ energyindv
counter=counter+1
End IF
End DO cheker
energy(m)=energytotal
counted(m)=counter
If(m<=Maxblocks)Then !display the resul

    write(10,2002)((p+29)/2.0 - 0.25),(k/2.0 -0.25),energy(m)

    2002 FORMAT (1X,F12.3,5X,F12.3,5X,ES14.4)

    site(l,p)=energy(m)

    End If
k=k+1 ;m=m+1
End Do column
q=q+1 ;m=m+1
End Do row
!.....
OPEN(UNIT=7,FILE='output',ACTION='write',Status='replace') !to see the out put
martix form
DO l=0,40
DO p=30,76
WRITE(7,100)site(l,p)
100 FORMAT (1X,ES10.4,)
End DO
WRITE(7,101)
101 FORMAT (/)
End Do
CLOSE(7)
END PROGRAM ENERGYMAPPING
```

7.4 Appendix D ...New located events in this study

New located events in this study

DATE - Date of the event (year/month/day)
OR. TIME - Event origin time in GMT (Hour:Minute:Second)
LAT. - Latitude of the earthquake epicenter in degrees
LON. - Longitude of the earthquake epicenter in degrees
MC.- Coda magnitude
DEP.- Depth in km
NST.- Number of stations used
RMS.- Root mean square error

Table 7.2 below shows new located events in this study.

7.5 Appendix E ...Poorly located events in Brazier et al., 2006

Poorly located events (events with less than 3 stations) by Brazier et al., 2006

DATE - Date of the event (year/month/day)
OR. TIME - Event origin time in GMT (Hour:Minute:Second)
ST.NA.- Station name used
NO.EV.- Number of events
Table 7.3 below shows poorly located events in this study.

DATE	*OR.TIME*	*LAT.*	*LON.*	*DEP*	*NST*	*RMS*	*MC*
00/08/30	11:19:37	9.423	38.668	0	3	0.8	3.2
00/09/12	17:41:42	11.302	36.958	28.6	4	0.4	2.8
00/09/28	17:58:41	10.492	41.801	0	5	1.3	3.1
00/11/17	04:34:11	7.553	38.396	0.1	3	0.7	2.7
01/05/12	02:46:54	9.442	39.802	0	5	1	2.1
01/05/12	04:00:54	9.123	39.833	0	6	0.4	1.2
01/05/14	05:16:06	9.278	39.667	0	3	0.4	2.1
01/05/24	21:25:52	9.359	40.28	3	5	0.5	2
01/05/30	20:19:14	9.192	39.983	3	5	0.8	2.1
01/06/04	11:38:27	9.262	40.266	0	6	0.8	2.4
01/06/08	05:00:03	11.876	39.735	6.2	4	0.1	1.8
01/06/22	11:27:05	9.138	40.444	0.1	4	0.6	1.7
01/06/22	14:09:20	8.613	40.293	0	4	0.9	2.8
01/06/23	19:12:07	9.275	40.394	0.9	5	1	3.4
01/06/24	07:26:37	9.206	40.45	0	5	1	2.5
01/06/24	18:17:28	9.177	40.443	0	6	0.6	2.1
01/06/25	08:26:19	9.285	40.158	0	7	0.6	2.9
01/06/25	16:39:51	9.096	40.281	30	5	0.7	2.1
01/06/25	16:52:57	9.387	40.387	3	4	0.7	2.5
01/06/27	10:40:14	8.748	40.247	40.9	3	0.5	2.8
01/06/28	07:13:43	8.483	39.69	0	4	0.2	2.7
01/07/17	18:27:21	13.129	39.024	163.8	5	0.6	2.5
01/07/26	20:20:56	9.957	39.716	8.3	3	1.1	2.3
01/08/04	11:51:09	9.22	40.306	0	3	0.5	1.1
01/09/02	13:08:55	9.443	39.799	0	7	0.9	2.1
01/09/08	07:57:18	9.497	39.975	3	3	0.2	2.1
01/09/08	11:24:11	9.677	40.42	0	3	0.7	2.5
01/09/13	9:37:02	10.331	39.935	0	4	0.4	2.1
01/09/13	17:51:28	10.279	39.748	0	5	0.3	3.2
01/10/20	20:50:51	9.312	39.893	0.1	3	0.5	1.7
01/10/22	04:35:46	10.496	40.003	0	3	0.6	2.4
01/10/22	15:11:32	9.72	39.786	1.7	5	0.7	3.2
01/10/24	02:26:55	9.125	39.873	0	6	1.3	3.1
01/12/24	08:33:52	12.413	40.501	13.3	3	0.1	3
02/01/08	22:18:38	9.588	39.589	2.9	3	0.6	2.3
02/01/17	20:07:36	9.501	39.792	0	4	1	2.2
02/01/18	15:43:26	8.083	40.071	110.9	4	1.1	2.5
02/02/07	18:44:41	10.512	39.612	0	9	1	3.1
02/02/11	13:56:38	9.407	39.118	0.1	3	0.4	4
02/02/13	00:38:22	9.256	41.315	2	3	0	2.9
02/02/13	08:48:05	12.805	38.342	0	4	0.4	3.8
02/02/13	23:25:53	11.841	42.485	0	5	0.8	2.7
02/02/17	02:38:12	9.502	39.949	0	4	1	2.4

DATE	*OR.TIME*	*LAT.*	*LON.*	*DEP*	*NST*	*RMS*	*MC*
02/02/17	02:42:15	9.168	39.933	0	4	1	1.9
02/02/21	08:21:59	7.392	38.611	0	7	0.8	1.9
02/02/25	20:45:33	9.772	39.859	2.8	3	0.9	1.7
02/04/24	23:23:59	6.87	38.719	2.8	3	0.5	2.3
02/05/14	18:49:31	12.141	41.615	0.1	4	0.3	2.2
02/05/16	21:09:56	13.461	40.843	0	3	0.2	2.9
02/05/18	2:00:09	13.409	40.342	29.2	5	0.1	3.5

Table 7.2: New located events in this study

DATE	*OR.TIME*	*ST.NA*	*NO.EV*
01/05/11	17:30:35	HERO	1
01/05/21	21:13:38	DMRK,HOSA	2
01/06/25	00:42:31	DMRK	1
01/08/21	01:44:45	HOSA	1
01/08/24	22:10:44	TEND	1
01/09/13	00:30:40	HIRN,HOSA	2
01/04/10	12:31:11	TEND	1
01/05/10	23:05:44	HOSA,JIMA	2
01/10/15	21:59:17	HOSA,JIMA	2
01/10/01	00:48L51	HOSA,JIMA	2
01/11/21	01:07:32	TEND,HOSA	2
01/11/22	19:13:54	TEND	1
01/11/23	00:34:01	TEND	1
01/11/24	22:16:46	DIYA,TEND	2
01/11/25	10:11:34	TEND	1
01/11/27	20:45:51	DIYA.TEND	2
01/11/27	20:49:29	DIYA.TEND	2
01/11/30	06:47:21	TEND,HIRN	2
01/12/07	22:56:33	TEND	1
01/12/01	19:41:43	ARBA	1
01/12/27	16:44:58	SELA,HERO	2
01/12/28	21:34:55	BIRH,WASH	2
01/12/31	00:07:16	BIRH	1
01/12/31	01:58:22	BIRH,WASH	2

Table 7.3: Poorly Located Events in this study.

7.6 Appendix F ...Location of the events in this study.

Fig 7.2 shows location of the events by this study for the time period 2000 - 2002.

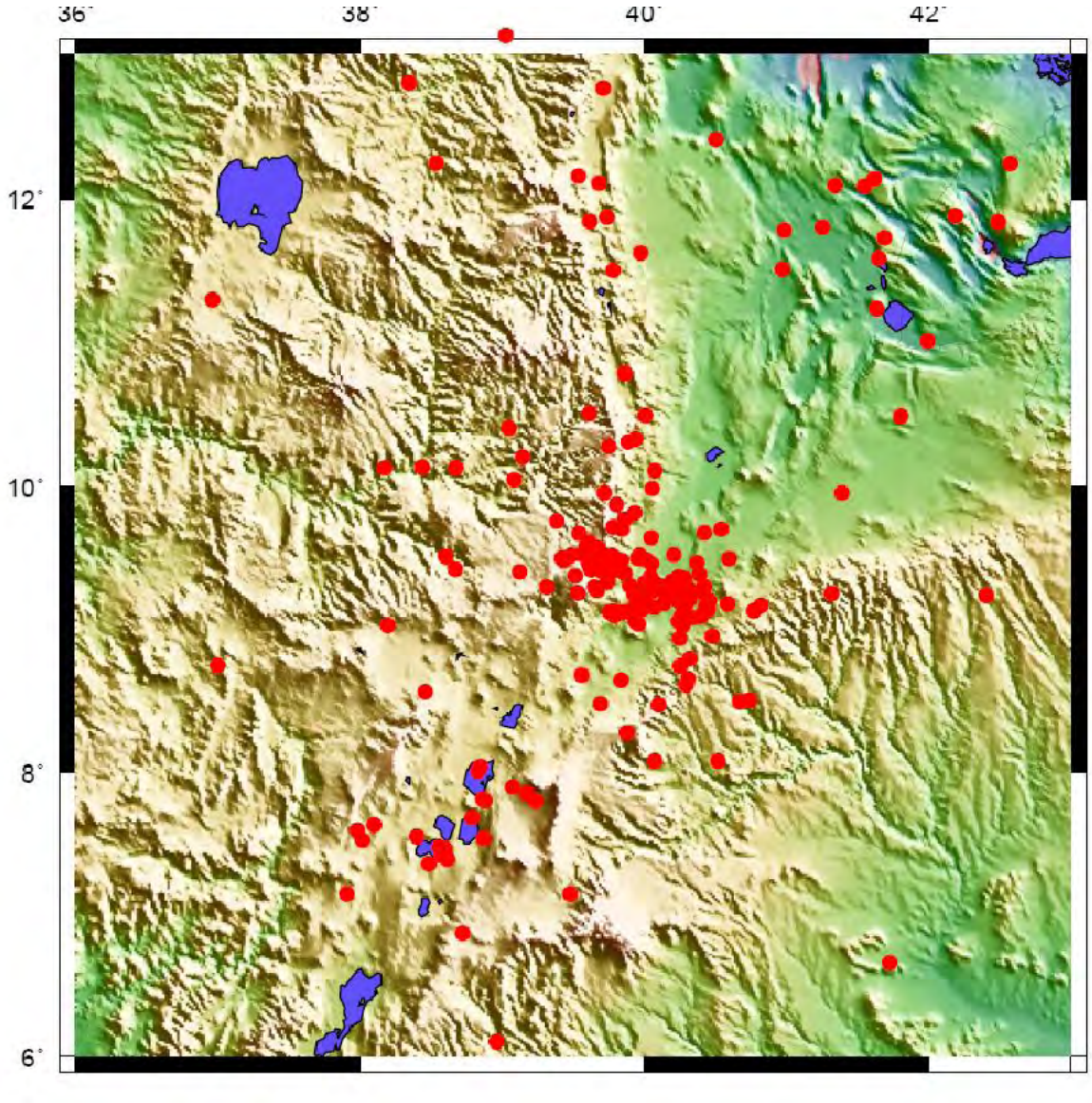

Figure 7.2: Locatioins of epicnenters determine for the period between 2000 and 2002. The red circles mark epicentral locatioins determined in this study

7.7 Appendix G ...locations of the events by Brazier et al.

Fig 7.3 shows Brazier et al., 2006 locations of the events from 2000 - 2002.

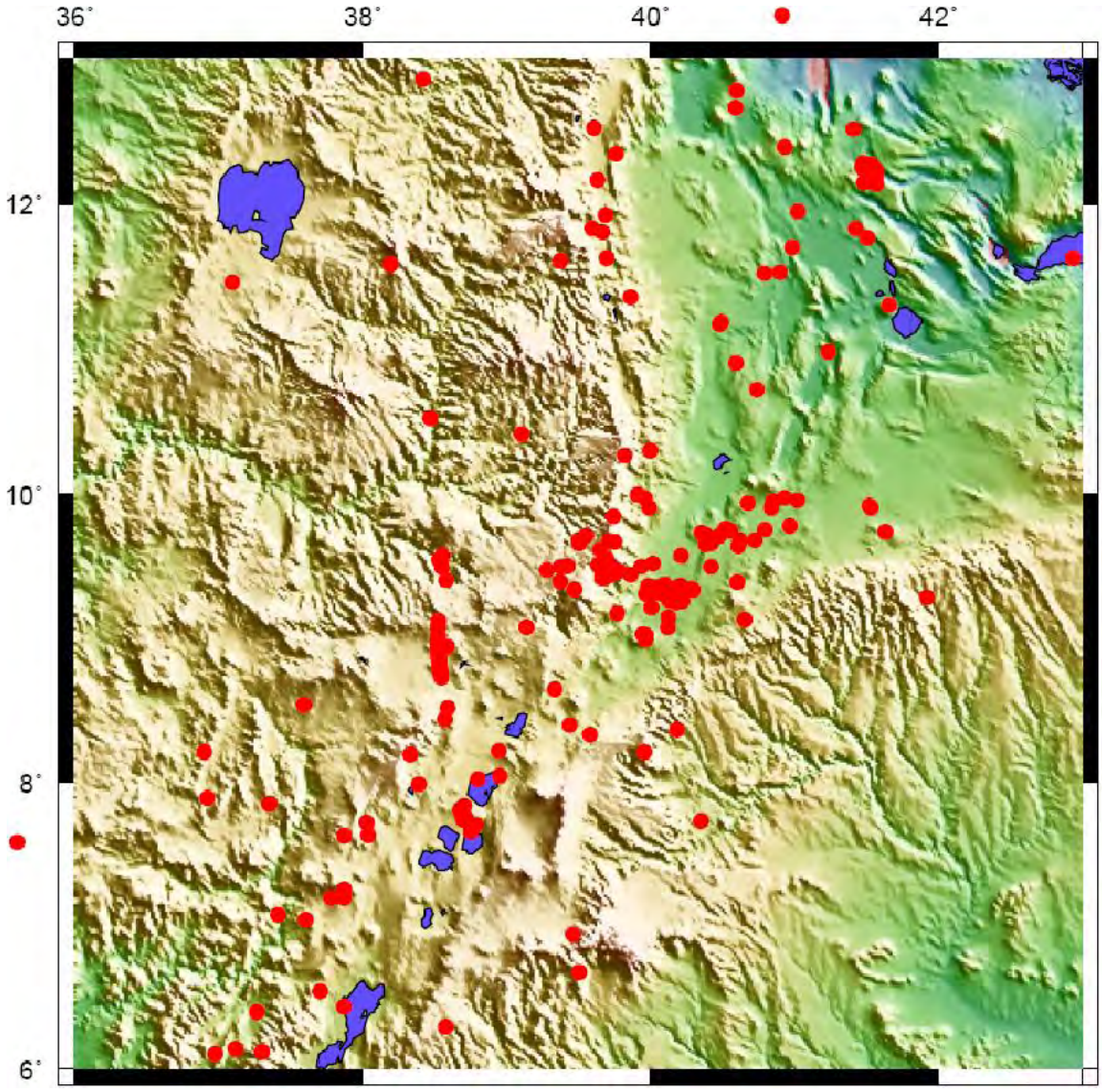

Figure 7.3: Brazier et al., 2006 locatioins of epicnenters determine for the period between 2000 and 2002. The red circles mark epicentral locations.

Declaration

I, Sisay Alemayehu, declare that this thesis is my original work and has not been presented for a degree in any other university, and that all sources of the material used for the thesis have been duly acknowledged.

Dr. Atalay Ayele (Advisor)
Signature

Sisay Alemayehu
Signature